

Chapter 5

Nanoparticle Behaviour in Complex Media: Methods for Characterizing Physicochemical Properties, Evaluating Protein Corona Formation, and Implications for Biological Studies



Wye-Khay Fong, Thomas L. Moore, Sandor Balog, Dimitri Vanhecke, Laura Rodriguez-Lorenzo, Barbara Rothen-Rutishauser, Marco Lattuada and Alke Petri-Fink

Abstract The transformation of nanoparticles (NPs) in physiological milieu is a dynamic phenomenon that is the subject of intense investigation. When introduced into the body, NPs can undergo a variety of changes, such as, protein adsorption, dissolution, agglomeration/aggregation, structural deformities and redox reactions. It is these changes that subsequently determine the uptake, bioavailability, translocation and fate of NPs, which ultimately determine their therapeutic efficiency, diagnostic efficacy or toxicity. This chapter will consider the colloidal interactions at the interface of NPs with the contents of biological milieu, the practical and theoretical considerations required to modify analytical and imaging techniques to detect and, if possible, quantify NPs in this complex environment, and the requirement for a highly interdisciplinary approach to understand the behaviour at the bio-nano interface.

W.-K. Fong · T. L. Moore · S. Balog · D. Vanhecke · L. Rodriguez-Lorenzo · B. Rothen-Rutishauser · A. Petri-Fink (✉)
BioNanomaterials, Adolphe Merkle Institute, Chemin des Verdiers 4,
1700 Fribourg, Switzerland
e-mail: alke.fink@unifr.ch

L. Rodriguez-Lorenzo · M. Lattuada
International Iberian Nanotechnology Laboratory, Water Quality Group,
4715-330 Braga, Portugal

A. Petri-Fink
Department of Chemistry, University of Fribourg, Chemin du Musée 9,
1700 Fribourg, Switzerland

Abbreviations

AFFF	Asymmetric flow field-flow fractionation
AFM	Atomic force microscopy
AUC	Analytical ultracentrifuge
BSA	Bovine serum albumin
BSE	Backscattered electrons
CD	Circular dichroism
CCM	Cell culture media
DC	Disc centrifuge analysis
DDLDS	Depolarized dynamic light scattering
DLS	Dynamic light scattering
DLS-zeta potential	Laser-Doppler velocimetry
EELS	Electron energy loss spectroscopy
ESEM	Environmental scanning electron microscope
EXAFS	Extended X-ray absorption fine structure
FBS	Foetal bovine serum
FCS	Fluorescence correlation spectroscopy
FRET	Förster resonance energy transfer
LIT	Lock in thermography LM: light microscopy
NPs	Nanoparticles
SANS	Small-angle neutron scattering
SAXS	Small-angle X-ray scattering
SE	Secondary electrons
SERS	Surface-enhanced Raman spectroscopy
SLS	Static light scattering
SPIONs	Superparamagnetic iron nanoparticles
sSAXS	Synchrotron small angle X-ray scattering
STEM	Scanning transmission electron microscope
STXM	Scanning transmission X-ray microscopy
TDA	Taylor dispersion analysis
TEM	Transmission electron microscopy
TiO ₂	Titanium dioxide
TRPS	Tuneable resistive pulse sensing
UV-Vis	Optical extinction spectroscopy in the UV-Visible range
XAS	X-ray absorption spectroscopy
XANES	X-ray absorption near edge structure
XRD	X-ray diffraction
XRM	X-ray microscopy
ZnO	Zinc oxide

5.1 Introduction

The unique properties of nanoparticles (NPs) have provided the opportunity for the creation of materials with properties that far surpass the bulk material. These materials, in turn, can influence and interact with biological systems on the colloidal (sub-micron) level. The successful application of nanotechnology has can be found in both industrial and biomedical settings, for instance, in the case of nanomedicine the safety and efficacy of the drug is determined by the properties of the NP, not the encapsulated drug [1, 2].

Although the promise and potential of NPs to significantly improve the quality of life is immense, the limited success of NPs from the plethora of academic literature is staggering. Whilst we are able to understand the behaviour of these engineered NPs in ideal conditions, it is more difficult to “observe” NPs behaviour in physiological media. This begs the question, how do we observe and quantify how the NPs are behaving in actuality?

Upon exposure to physiological fluids, NPs undergo a variety of colloidal interactions with different components, specifically, salts, sugars and proteins. This interface between the ‘bio-nano’ comprises the dynamic physicochemical interactions, kinetics and thermodynamic exchanges between nanomaterial surfaces and biological components. These interactions can have a devastating effect on the stability of the NPs in vivo. Fundamental physical chemical studies are generally performed in ideal conditions in order to maintain the integrity of the particle design and conjugation,

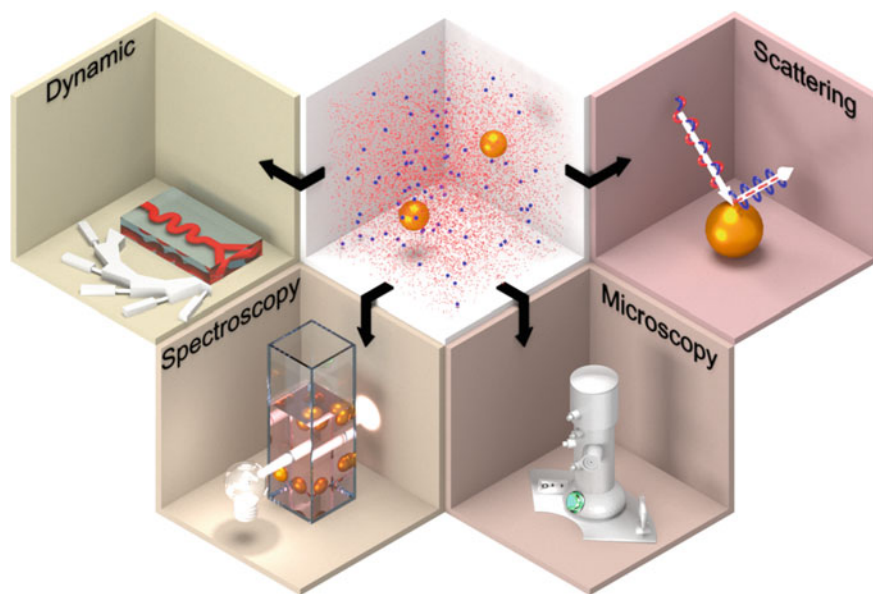


Fig. 5.1 Nanoparticles in complex fluids undergo multiple interactions when they encounter physiological fluids. These interactions can be illuminated and investigated by multiple techniques

however it is the alterations to the particle when exposed to physiological fluids that ultimately determine the biocompatibility and biodistribution of these particles [3].

The purpose of this chapter is to promote interdisciplinary communication between the physical chemistry and the biology communities concerning the development of NPs for bio-applications. In the first instance, the physiological challenges to NP stability will be briefly explored. Then, this chapter will explore the life of NPs in complex media that mimic *in vivo* environments. Thus, the following topics will be explored: physiological milieu as complex, crowded fluids; the potential influence of complex environments upon NP; current and emerging methods that are available to assess NP stability; and how to translate this data to help develop NPs from bench top to the clinic. Discussion surrounding methods is split into four foci: scattering, spectroscopy and separation, microscopy and dynamic methods (Fig. 5.1).

5.2 Biological Fluids: Composition as Colloids

In a biomedical context, NPs will enter a number of “complex” environments when administered *in vitro* or *in vivo*. *In vitro*, the most common solution NPs will encounter is cell culture media (CCM), which usually contains foetal calf or bovine serum required for optimal cell growth. Depending on the biomedical application of the particle system, it may be necessary to test their performance and behaviour in simulated physiological solutions. Finally, for particles that are introduced into the

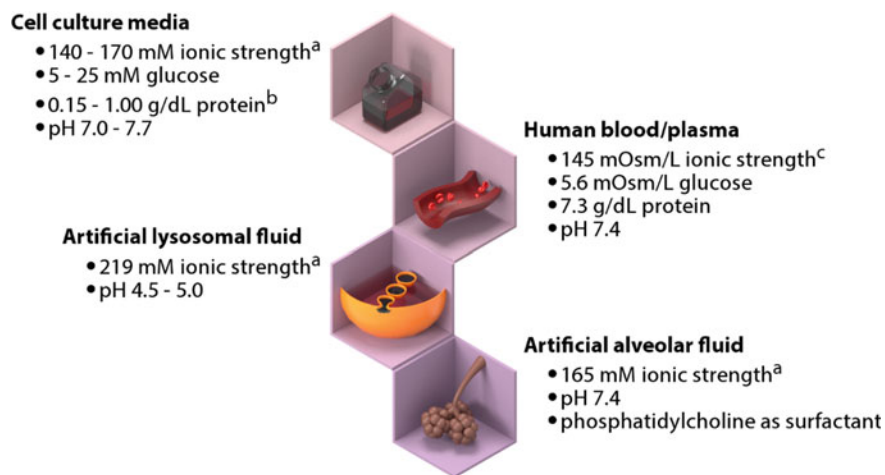


Fig. 5.2 Biological media are comprised of cell culture media, physiological fluids (i.e. human blood or plasma), as well as various synthetic/artificial fluids. These solutions can vary significantly in their composition and thus impact their effects on NP. ^a Estimated based on the inorganic salt concentrations in the media composition assuming no protein interactions in supplemented media; ^b assuming a 5–20× dilution of standard foetal bovine serum into cell culture medium; ^c estimated from the ion concentrations provided by [4]

human circulatory system, understanding what NPs may encounter in whole blood or plasma is critical to inform the rational design of particle systems. The human body comprises many dynamic solutions where biomacromolecules, ionic strength, changes in pH, and active biological processes can act to (de)stabilise, dissolve, and transform particles. In order to assess the effect of biological and physiological fluids on particles, it is therefore important to understand the composition of these fluids, where some of the differences are summarised in Fig. 5.2.

5.2.1 Cell Culture Media

There are a wide range of CCM, where Yao and Asayama have provided an excellent review of their history and use [5]. Synthetic CCM are comprised of a mixture of inorganic salts, amino acids, vitamins, and sugars. Media was initially derived from natural physiological solutions (e.g. blood plasma). The findings that cell proliferation could be improved by exchanging the CCM [6] or adding extracts from physiologically relevant fluids to the growth media [7] instigated a search to understand what biological components led to successful cell culture. Fischer first pioneered a method to understand the necessary components of CCM for cell viability and growth by using a dialysed serum that controlled the amount of low molecular weight components (amino acids, vitamins) added [8].

Initial attempts at CCM were comprised of balanced salt solutions, primarily inorganic salts that were possibly supplemented with glucose [5]. Research in the past century has resulted in the development of numerous “basal” media, that is, CCM containing the minimum essential components to promote cell growth, including proliferation and differentiation. Thus, these balanced salt solutions and basal media are high ionic strength solutions that can have an adverse effect on particle stability. In the presence of high ionic strength solutions, the electrical double layer of NPs can be compressed, resulting in particle colloidal destabilisation and aggregation [3]. If only accounting for the contribution of inorganic salts and not factoring potential interactions of salt ions with biomacromolecules, the ionic strength of basal media can vary between 140 and 170 mM.¹ Thus, NPs need to have mechanisms to prevent aggregation due to high salt content.

These basal media are commercially available, and for conventional cell culture they are traditionally supplemented with protein-rich serum such as foetal bovine serum (FBS) or pooled human serum, generally at a rate of 5–20%. This equates to a protein concentration of approximately 0.15–1.00 g/dL [9].

Generally, basal medias are also buffered to maintain pH of 7.4, but optimal cell growth pH can vary between 7.0 and 7.7 [10]. Changing pH can have dramatic ramifications on particle colloidal stability. Usually, the isoelectric point of the NP material will in part dictate particle surface charge, and changing pH can alter the particle surface charge, which can in turn stabilise or destabilise NPs.

¹Based on inorganic salt concentrations of several common basal media formulations, such as DMEM, MEM, RPMI-1640, DMEM/F-12, Medium 199 with Earle's salts.

5.2.2 *Model Physiological Fluids*

In some cases, model physiological fluids are employed in order to mimic certain biological environments. In the context of NPs for biomedical applications, by studying NP behaviour in these fluids, realistic particle behaviour can be examined, such as dissolution/degradation, aggregation, release of active pharmaceutical ingredients, and targeting efficiency. These include artificial lysosomal fluid (ALF), artificial alveolar fluid, artificial synovial fluid, artificial interstitial fluid, and artificial gastric juices. The composition of these artificial biological fluids vary based on pH, inorganic salt concentrations, and presence of other biopolymers [11]. For example, ALF, meant to mimic the endo-lysosomal compartments of cells through which most NPs will be trafficked upon internalization, has a pH from 4.5 to 5.0. Artificial gastric juices, which mimic stomach acid, have a pH even lower at 1.5. These low pH values can severely degrade or dissolve NPs, thereby destabilising them. Moreover, varying salt concentrations can act to destabilise particle solutions.

5.2.3 *Human Blood and Plasma*

When considering NPs entering the body, blood is the primary tissue with which these particles will first come into contact. Blood comprises of approximately 7% of a person's body weight (~5 L) [4], which is in turn comprised of 60% plasma (water, proteins, glucose, clotting factors, and electrolytes) and 40% red blood cells (RBCs). Plasma contains high concentrations of sodium and chloride ions (142 and 108 mOsm/L, respectively), as well as a mixture of proteins (6.4–8.3 g/dL) [12] that are mostly comprised of serum albumin, immunoglobulins, receptor ligands, and tissue leakage proteins [13]. Blood also contains assorted phospholipids (0.28 g/dL) and cholesterol (0.15 g/dL), macromolecules with the potential to adsorb onto NPs and in part mediate their biological fate [14]. Human blood has a tightly regulated pH at 7.4, however certain pathological conditions can result in acidosis or alkalosis [15].

The cellular component of blood could also factor into particle interactions within this biological space. RBCs vastly outnumber leukocytes, the immune cells responsible for defending against foreign pathogens, at approximately 700:1. However, leukocytes play a major role in mediating NPs fate in the body. The cellular components of blood (e.g. RBCs and leukocytes), may interact with particles that are introduced into intravascular flow. Upon introduction to blood, opsonin proteins can adsorb onto the particle surface—these proteins act as ‘flags’ for leukocytes to sequester particles from circulation and tissues [16]. Some have even exploited the potential of naturally circulating cells to transport NPs to physiological targets [17, 18].

5.3 Fate of NPs in Electrolyte and Protein Crowded Environments

NPs are similar in size to intra- and extracellular biological species, which can result in interactions with biological components such as cells and proteins, thereby affecting cellular processes. This has two major consequences: firstly, it makes them very attractive candidates for medical applications; secondly, the increasing use of engineered NPs has raised serious concerns about their safety for human health and the environment. Both nanomedicine and nanotoxicology are complementary disciplines aimed at the prevention and treatment of diseases, which require the development and/or study NPs in *physiological environments*.

The behaviour of the NPs and their potential physiological impact are determined by the physicochemical properties of the particles (such as size, surface, crystallinity, shape etc.) and the interaction with their environment. Due to the complexity of the environment, it is almost impossible to predict particle behaviour in a particular cell or physiological medium [19]. Thus, it is crucial to first discuss the most prominent possible consequences arising from NP incubation in complex biomimetic and/or physiological fluids (Fig. 5.3).

Particle aggregation

Once the NPs are incubated in complex physiological fluids, their surfaces are exposed to significant amounts of salts, proteins, vitamins etc. This encounter can induce NP aggregation (see previous chapter), which is a common phenomenon and has important consequences with for the particles and the cellular dose [3]. In a study comparing carbon nanotube aggregates with bundles of the same carbon nanotubes, Wick et al. has correlated the dispersion state to the cytotoxicity of the material [19]. Teeguarden et al. showed that 15 nm silver NPs appear ca. 4000 times more potent than a micron sized particle on a cm^2/mL media basis [20]. Albanese et al. studied the impact of NP aggregation on particle uptake and cytotoxic behaviour. They could not show unique toxic responses but were able to correlate uptake patterns with particle aggregation [21].

Nanoparticle dissolution

As the size of a material decreases, its surface area and volume decrease. However, the surface area to volume ratio will develop by a ratio of $3/r$, with r being the radius. Consequently, an increased number of all atoms that constitute the particle will be surface atoms. NP size and surface area to volume ratio, respectively, influence particle dissolution kinetics. Typically, a decrease in particle size correlates with an increase in particle dissolution [22]. Although the underlying mechanisms responsible for this inverse correlation are not yet fully understood, it is widely accepted that (a) aggregation decreases dissolution and (b) metal NPs can undergo oxidative dissolution [23]. However, several parameters play an important role and are often hard to separate. For example, particle dissolution and consequently ion release was shown to correlate not only with particle size, but also with its shape,

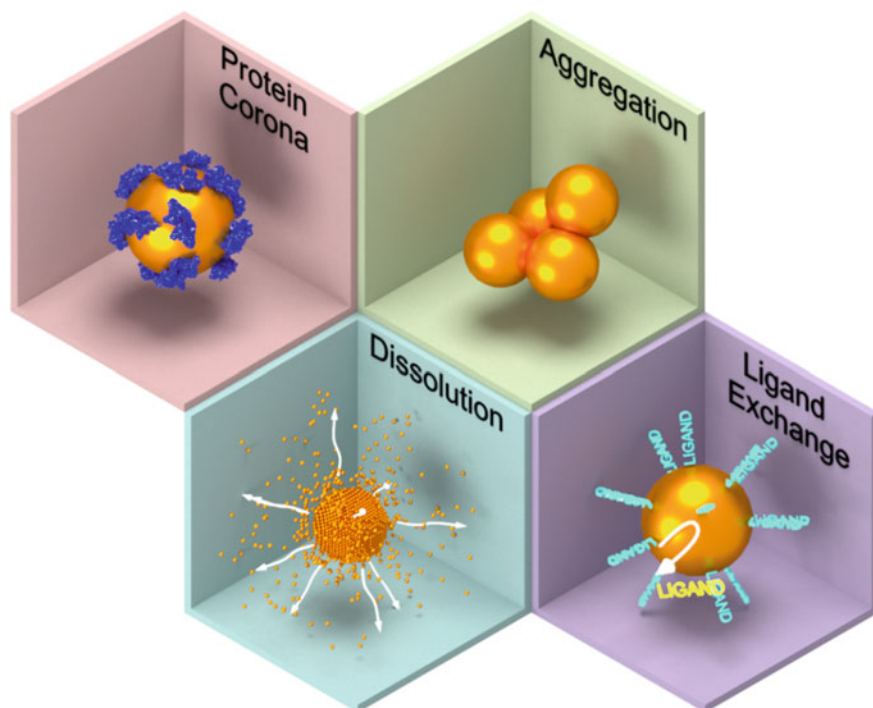


Fig. 5.3 Schematic illustration of possible consequences arising from nanoparticle incubation in physiological fluids. ^a Formation of protein corona which can both shield targeting moieties or antibodies as well as denature proteins; ^b nanoparticle aggregation; ^c nanoparticle dissolution; ^d removal or exchange of surface ligands

surface coating, in addition to environmental factors such as temperature, pH, ionic strength, dissolved oxygen, and the presence of proteins [24].

Removal or exchange of surface ligands

In many cases, anchoring ligands are not firmly chemically bound to the particle surfaces but ligand grafting relies on relatively weak interactions with the surface atoms of the particles. Consequently, it is imaginable that the presence of biomolecules (or high affinity ligands) could remove surface grafted ligands. For example, physiological concentrations of thiol-containing molecules such as cysteine have been shown to displace thiolated polyethylene-glycol from the surface of gold NPs [25]. The partial loss of the ligand, however, has far-reaching consequences as it impacts colloidal stability of the NPs, modifies the adsorbed protein profile, and ultimately results in the complete loss of biochemical or analytical function such as targeting ligands (e.g. antibodies), or fluorescent dyes [26]. Kreyling et al. attributed the degradation of a NP grafted polymer coating *in vitro* and *in vivo*, on proteolytic enzymes of endosomal and lysosomal cellular compartments [27].

5.4 Interaction with Biomolecules: The Corona of Proteins and More

5.4.1 *The “Protein Corona”*

The consequent fate of NPs is determined by how they react to biological components they encounter in physiological systems. Upon interaction with biological media (i.e. human blood/plasma, cell culture media, etc.), the surface of a particle will become rapidly opsonised, that is coated with biomacromolecules, in preparation for their removal by immune cells [28]. This forms the “protein corona,” a layer of tightly bound and immobile biomacromolecules (e.g. proteins) comprising the hard corona and a weakly associated mobile layer known as the soft corona [29]. The interaction of particles with biological systems is widely attributed to the physicochemical characteristics of the NP; that is, the size, surface charge, surface functionalisation, shape, and material. However, because the protein corona forms a biological layer around particles, it is fair to state that physicochemical characteristics drive nano-bio interactions through the protein corona. In fact, work done by the group of Warren Chan has shown that the protein “fingerprint” (i.e. characteristic NP protein corona) is the optimal indicator for predicting particle-cell interaction [30, 31].

5.4.2 *Factors Affecting Protein Corona Formation*

The formation of the protein corona is driven by particle physicochemical characteristics at the particle surface [32]. When particles are introduced into a biological fluid, proteins will adsorb rapidly onto their surface due to van der Waals interactions, Columbic forces, hydrophobic interactions, and hydrogen bonding. Protein adsorption can result in changes to the protein conformation or alter protein solubility, which can have major consequences on protein function by altering their secondary and tertiary structures [33–35]. Significant research has been pursued in order to understand how particle physicochemical characteristics influence protein corona formation, and several excellent reviews on the particle protein corona exist [36, 37].

The formation of the corona is not only driven by physicochemical factors, but also experimental conditions such as experimental temperature, exposure time, particle concentration, and method of isolating particles for analysis [37–39]. However, in the most basic sense, the formation of the protein corona is a study of protein interactions with a (nano) surface. An early study by Lück et al. [40] showed that latex particles with different surface charge densities altered protein adsorption, and Gessner et al. [41] likewise investigated the effect of different surface chemistries on corona formation around latex particles. They showed that Columbic interactions between the particle surface functional groups and proteins were a critical in determining protein corona formation. Tenzer et al. [42] investigated the effect of particle

size, surface charge, and incubation time on the formation of protein corona on silica and polystyrene NPs in human plasma. They observed that the protein corona forms rapidly (~30 min) and remains rather consistent over time. Isolating particles at time points earlier than 30 min, where there may be protein exchanging between abundant proteins and higher affinity proteins (i.e. the Vroman effect) [43, 44] is a non-trivial challenge. A study investigating polystyrene particles with different functional groups (carboxy, amino, sulfonate, and phosphonate) showed that amino and sulfonate groups enriched the adsorption of apolipoproteins; proteins that can reduce the uptake by phagocytic cells and so prolong circulation time [45]. Thus, Coloumbic and hydrophobic interactions, dictated by the particle material and surface functionalisation, seem to be the key drivers mediating protein corona formation.

Often, polymers are chemically coupled or adsorbed to particle surfaces to enable a so-called “stealth” effect [46]. Poly(ethylene glycol) (PEG) is the gold standard for particle shielding, reducing particle clearance and prolonging blood circulation time while reducing the adsorption of opsonins (which facilitate particle clearance). Interestingly, it seems that the protein corona, and not merely reducing protein adsorption due to polymer shielding, is responsible in the stealth effect observed with polymers such as PEG or poly(ethyl ethylene phosphate) [47]. It has been shown that PEG conformation on a particle surface in part mediates particle circulation time in vivo [48], and other evidence shows that this could be due to variations on the protein corona based on PEG conformation [49]. Furthermore, PEG chain length and surface coverage dictate protein corona formation (and subsequent biological interactions) in part [50]. The use of other stabilising molecules (e.g. surfactants, which can adsorb onto particles via hydrophobic interactions, electrostatic or van der Waals forces) has also been shown to mediate protein corona formation [51, 52].

Particle size has been investigated for its role in mediating protein corona formation; however, results vary as to what effect size has. Cedervall et al. [29] showed that the total amount of protein adsorption onto polymeric particles was determined by size (scaling with the amount of particle surface available), however the pattern of proteins adsorbed remained consistent. A study on different sized gold NPs (5, 15, 80 nm) showed that protein corona composition changed across the different size regimes [53]. Thus, it appears that particle size (largely due to the amount of surface area and also the material) can play a role in corona formation but the effect is not consistent. Similarly, particle shape may influence protein corona formation. Miclăuș et al. [54] showed that protein adsorbed preferentially to silver nanocube faces as opposed to edges at early time points (<1 h), though it is unclear if this difference is due to the particle geometry or due to displacement of particle-stabilising polyvinylpyrrolidone which has a different affinity to the particle surface depending on the crystal plane to which it is adsorbed. However, another study showed via 2D gel electrophoresis that there was a difference in protein adsorption onto titanium dioxide nanoparticles, nanorods, and nanotubes, i.e. due to particle shape [55].

It is difficult to draw any type of universal guiding rule for protein corona formation; rather particles are currently investigated on a case-by-case basis noting the particle material, surface functionalisation/properties, shape, size, etc. However, it

is possible to make some predictions for particle interaction with biological systems based on the bimolecular corona.

5.4.3 Beyond Proteins: Other Components of the Corona

Lipids, sugars, vitamins and other small organic molecules can or may also adsorb on the NP surfaces, thereby affecting immunogenicity and potentially hampering targeting abilities of administrated NPs, and in part mediating nano-bio interactions [51, 56]. For example, Müller et al. [51] showed that the lipid-domains of lipoproteins were also responsible for adsorption processes, indicating that lipid-like molecules can comprise the protein corona. These data are supported by the fact that surfactants and hydrocarbons are often used to adsorb stabilising macromolecules, ligands, and polymers onto particle surfaces [52, 57]. Studies on lipoprotein binding onto hydrogel particles revealed that high-density lipoproteins and, cholesterol, and triglycerides are present in the bimolecular corona, and are speculated to govern particle interaction with, for example, lipid transport pathways [14]. Investigations into the glycosylation of proteins, the natural and frequent modification of proteins with sugar molecules, showed that protein coronas that were deglycosylated (i.e. sugar molecules removed from corona proteins) were less stable and increased the adhesion of particles to cells [58]. It is therefore evident that biomolecules beyond proteins may yet play an important role in our understanding of fundamental bio-nano interactions.

5.4.4 Biological Effects of the Protein Corona

Even after extensive characterisation *ex vivo*, the eventual biodistribution of the NP plus biomacromolecule corona can result in unexpected *in vivo* behaviour. This rearrangement has been shown to affect their pharmacological activities, interaction with their environment (i.e. other proteins) and other biological responses [59, 60].

When the NP reach their target, it is the corona that the cells actually ‘see’. The corona may contain opsonins, which can enhance the uptake of the NP-corona-complex by cells of the reticuloendothelial system (RES) [61, 62]. This “molecular signature” is recognised by immune cells and so determines the route of particle internalisation, its pharmacokinetics, namely, volume of distribution, organ disposition, and rate of clearance from the blood and body [63, 64]. Recent studies have also demonstrated that surface adsorbed biomolecules can shield NP functionality, reduce cell selectivity [65] and impact cellular uptake kinetics [45]. Thus, the type and number of proteins that the NP attracts determines its biodistribution. It follows that there have been and continues to be a plethora of studies and reviews into understand exactly what physicochemical properties of different kinds of NPs determines the composition of their protein corona [3, 66].

In terms of biocompatibility, the formation of the corona can be advantageous or disadvantageous [67]. Attached biomacromolecules that are not recognized by any receptors make the particle less attractive to the cell. For example, Salvati et al. demonstrated that proteins can shield NP derivatised transferrin from binding to its receptors on cells and entirely lose its targeting specificity [68]. On the other hand, if a developed corona contains the right biomarkers, they can activate the endocytic pathway of the target cell, where it consequently effects haemolysis, thrombocyte activation, nanoparticle uptake and endothelial cell death [42]. Several studies have demonstrated enhanced biocompatibility of protein coated NPs compared to the originally protein-free synthesised NPs [69]. For instance, the pre-coating of blood proteins on the surface of carbon nanotubes greatly alter their cellular interaction pathways and result in much reduced cytotoxicity [70]. In a landmark study, Wang et al. deliberately manipulated the corona of positively charged polystyrene NPs in order to traffic them into the lysosomal compartments of target cells [71]. In addition to the surface character of the single particles, aggregation also determines their biodistribution. This is elaborated upon in Sect. 6.5. As can be seen, it is insufficient to characterise NP designed for in vivo use solely in pristine conditions as the biological identity conferred onto the surface of the NP by the components of the corona determines their fate. Thus, in the following sections, methods to characterise the protein corona and their changing colloidal identities will be discussed.

5.4.5 Characterising the Protein Corona

Given the importance of the corona surrounding the NP, the investigation of its composition is key to understand the biological impact of nanomaterials. In general, the following processes are taken in order to characterise the NP-corona. Firstly, the NPs are incubated with the representative complex media of choice for a defined period. The complexes then have to be separated from the unbound proteins in the matrix. Different protocols achieve this by initially washing and centrifuging the sample, followed by further processing such as magnetic separation (limited to magnetic NP [72]), microfiltration, ultracentrifugation, chromatography and/or electrophoresis, where the latter two techniques allows for the exquisite and more gentle separation and isolation of NP-biomacromolecule-complexes from unbound components. Protein corona separation and characterisation is summarised below and in Table 5.1, and is reviewed in more detail in these informative references [37, 73–76].

5.4.5.1 Separation

Chromatography separates components based on the differences in their interactions with stationary phase of the column through which they are travelling. The main method to separate unbound biomacromolecules from the NP-corona is size exclusion chromatography (SEC), and to a lesser extent ion exchange chromatography

Table 5.1 Summary of the techniques that can be used to separate NP-corona complexes, characterise protein composition and protein conformation

Function	Technique	Advantages	Disadvantages	References
Isolation of NP-corona	Chromatography Field-flow fractionation Capillary electrophoresis 1D/2D gel electrophoresis	Quantitative Low shear force Quantitative Simple, fast	Limited applicability High complexity Limited sensitivity Limited separation	[29, 77, 78] [39, 79] [80–84] [85–91]
Characterisation of protein composition	Proteomics + mass spectroscopy	Quantitative, high resolution	Time consuming, expensive, significant experimental and theoretical expertise required	[29, 90, 94, 95]
Characterisation of conformational change	Fourier transform infrared spectroscopy Raman spectroscopy Fluorescence spectroscopy Circular dichroism Nuclear magnetic resonance spectroscopy Isothermal titration calorimetry	Identifies amide bands of proteins bound to NP Identifies amide bands of proteins bound to NP in solution Wide range of probes available Identifies secondary structures of proteins Can map site of protein attachment Kinetics and thermodynamics of protein attachment	Sample preparation destroys samples Autofluorescence and Raleigh scattering noise In vivo environment can adversely change signal Limited specificity Line broadening of spectra High sample concentration and user expertise	[96, 97] [98] [101] [103, 104, 110–112] [14, 105–107] [108, 109, 113]

(IEC) and reverse phase liquid chromatography (RPLC). SEC separates components based on size. Larger molecules are unable to interact with the stationary phase and thus move rapidly through the column, whereas smaller molecules such as unbound proteins are able to fall into the pores in the mobile phase and thus move slower through the column [29]. IEC separates components based on their affinity to the ion exchanger, where the elution of components can be easily manipulated by changing the ionic strength of the mobile phase [77]. RPLC separates components based on their polarity through their interaction with the hydrophobic stationary phase [78].

Recent studies have utilised flow field-flow fractionation to separate NP from protein solutions. Field-flow fractionation is a chromatography-like method that separates components in a fluid suspension or solution by applying a field (e.g. temperature, gravity, centrifugal) perpendicular to the direction of flow of the sample in a long and narrow channel. This causes separation of the components present in the fluid depending on their differing mobility under the force exerted by the field. This method allowed for the differentiation of the corona proteins on SPIONS based on their relative dissociation rates from the NPs [79]. A more advanced version of this technique, asymmetric flow field-flow fractionation (AFFF), is described in more detail in the Sect. 5.6.5. This method has a lower shear force on the sample and thus, remarkably, was able to keep the soft protein corona on a polystyrene NP intact for further analysis [39].

Electrophoresis separates proteins by their migration in an electric field depending on their electrophoretic mobility, size or charge. Most commonly, capillary electrophoresis (CE), 1D and 2D gel electrophoresis is used. CE separates components based on charge and friction and is performed in submillimetre diameter capillaries. It has been used to separate polymeric [80–83] and metallic NPs [80, 84] from the different components of plasma. 1D and 2D gel electrophoresis differ in complexity and sensitivity. 1D separation is simpler and faster to run and separates components through a polyacrylamide gel based on molecular weight, 1D gels can be used to detect between 1 and 50 ng for a single protein band. Whereas 2D provides higher separation of components as it separates components in a polyacrylamide gel based on molecular weight and isoelectric point. 2D gel electrophoresis is nominally used when protein mixtures are more complex. Gel electrophoresis has been widely used in order to separate a wide variety of particles from metallic NP [85, 86], liposomes [87], carbon nanotubes [88, 89] and polymeric particles [90, 91]. Images of the 2D gels can then be analysed via readily available software that compares the image to a 2D master map of human plasma proteins [76, 92] and/or linked with spectroscopic techniques described below.

5.4.5.2 Protein Quantification

Separation techniques are subsequently coupled with mainly spectroscopic methods in order to identify the composition and/or conformation of protein in the corona. Protein identification is achieved by mass spectroscopy (MS) and proteomics. MS ionizes chemical species and then sorts the ions based on their mass-to-charge ratio.

The MS spectra is then analysed and proteins identified via a database search [93]. Following the separation of the NP-corona-complex from free protein, the corona then needs to be separated from the NP. This is achieved by either the use of surfactants and subsequent separation using gel electrophoresis and then MS analysis of the fractions [29, 90, 94]; or by “shotgun proteomics” which is the in situ digestion of the NP-corona-complex by a protease (trypsin) followed by separation of the individual proteins and peptides by liquid chromatography MS [95]. Thus far, MS is the only method that can provide single protein identifications.

5.4.5.3 Protein Conformation

NP bound proteins can change their 3D structure when compared to the native proteins in solution, thus many techniques are used to investigate conformational change as an indication of binding to the NP.

Fourier transform infrared spectroscopy (FTIR) measures the wavelength and intensity of the absorption of infrared (IR) radiation by a sample. The absorption of IR radiation excites vibrational transitions in molecular bonds, where the vibrational frequency depends on the strength and polarity of the vibrating bonds, they are influenced by intramolecular and intermolecular effects. Protein molecules exhibit many vibrational frequencies and it is through identifying these vibrations that proteins conformation can be elucidated [96, 97]. In a similar manner, Raman spectroscopy (RS) identifies protein secondary structure by probing molecular vibrations to provide a molecular fingerprint of biomolecules at the surface of NPs [98]. When these proteins are adsorbed on plasmonic NPs, a surface-enhanced RS (SERS) effect occurs, enhancing the Raman signal, thereby allowing the study of the NP-protein complex at low concentrations. However, Raman and FTIR spectroscopy differ in some key fundamental ways. RS investigates changes in polarisability of a molecule, whereas IR spectroscopy looks at changes in the dipole moment. RS measures relative frequencies at which a sample scatters radiation, whereas FTIR measures absolute frequencies at which a sample absorbs radiation. FTIR spectroscopy is particularly sensitive to heteronuclear functional group vibrations and polar bonds, especially OH stretching in water. Raman on the other hand is sensitive to homonuclear (e.g. C–C, C=C and C≡C) molecular bonds.

Fluorescence spectroscopy is used to look at protein conformation as fluorescent signals are exquisitely sensitive to the immediate environment of the probe, have a high signal to noise ratio, and the time scale of emission is in the nanosecond range [99, 100]. This technique has been used to probe the kinetics of protein attachment [101].

Circular dichroism (CD) occurs as a consequence of the interaction of polarised light with chiral molecules. As proteins are chiral molecules, changes in the secondary structure of proteins can be identified via CD spectroscopy [102]. It is thus utilised for the rapid evaluation of structural and stability changes when the proteins form stable, noncovalent, complexes with NPs [103, 104].

Nuclear magnetic resonance spectroscopy (NMR) observes local magnetic fields around atomic nuclei. The intramolecular magnetic field around an atom in a molecule changes the resonance frequency, thus giving access to details of the electronic structure of a molecule and its individual functional groups, allowing for the observation of not only chemical identity, but also structure, dynamics, reaction state, and chemical environment of molecules. Thus, it has been used to observe the corona of liposomes [105], lipids in the corona surrounding polymeric particles [14], as well as hydroxyapatite surfaces [106]. On the flip side, a recent study has utilised ^{19}F diffusion NMR to look at changes in the hydrodynamic radii of gold NP upon exposure to complex media as opposed to changes in proteins attached to the NP [107].

The kinetics of protein attachment to NPs can be identified by isothermal titration calorimetry (ITC). ITC identifies the thermodynamic parameters (binding affinity, enthalpy changes and binding stoichiometry) of interactions in solution by measuring a change in heat upon the addition of a component to another one in solution. Consequently, it has been used to study the binding of proteins to particles [108, 109].

The protein corona is recognised as a critical factor in understanding fundamental interactions between nanomaterials and biological systems. Whether exposing particles to cells, injecting particles into a living organism, or evaluating the effect of particles on an ecosystem, the biomolecular or protein corona will serve as the interface between nanomaterial and biology. Within this chapter we focus on the characterisation of particles in complex biological media, and there is simply not enough space to cover the complex and nuanced depth of the protein corona topic. For that the readers are directed to several excellent reviews mentioned in the beginning of this section. However, it is important to understand that the protein corona will drive the interaction of particles with a biological system, and so mediate particle colloidal behaviour (i.e. colloidal stability/aggregation, cellular interaction, etc.). One crucial aspect of corona formation is its impact on colloidal stability, where the presence of proteins can either enhance or reduce colloidal stability, the following sections of this chapter will discuss the colloidal behaviour of NP in more detail and how it is analysed.

5.5 Theoretical Considerations with Regards to Colloidal Stability in Physiological Media

5.5.1 Fundamentals of Nanoparticle Aggregation

Given that the behaviour of a NP cannot be decoupled from its surroundings, describing NPs in the context of their actual environment is crucial. For example, while particles may quickly aggregate in water, they may become completely stable in CCM, due to the high excess of proteins that alters particle interactions and stabilises the dispersion [114]. The opposite of this is also frequent, and NP aggregation is immi-

ment as soon as particles dispersed in CCM [115]. In both cases, the resulting protein covered NPs have completely differently physical properties from individual NP. Consequently, experimental characterisation must give an accurate account of several fundamental properties regarding the chemical and physical behaviour of the NPs, as it is these properties that influence their efficacy [116], specifically:

- chemical composition of the core and surface
- surface charge
- density and conformation of functional groups
- phases found in/on the particle (amorphous vs. crystalline phases)
- porosity, structure of porosity (fractal vs. ordered)
- size and its distribution
- shape and its uniformity/heterogeneity
- colloidal stability in terms of aggregation
- physical stability and chemical integrity (dissolution, ligand exchange)
- optical and magnetic properties.

Therefore, characterisation should be performed in both in ‘ideal’ conditions and in complex CCM. Interested readers are directed to several reviews introducing the available techniques briefly introduced below for the physicochemical characterisation of NPs in complex biological media [117, 118].

5.5.2 Consequences of Nanoparticle Aggregation on Cell Studies: Dosimetry of Single Particles Versus Aggregates

The influence of NPs internalized by cells is frequently studied by using in vitro models. In these models, establishing dose–response relationships are of paramount importance, where the metrics of the administered dose are NP number, mass, volume, and surface area. Due to the nature of cell culture experiments, the dosimetry metrics must be ascertained at three different sites: the dose administered to the cell culture, the dose delivered to the cell surface, and the dose internalised by the cell, whereas the two latter are the most relevant for the subsequent cellular interaction and induction of responses [119, 120]. The measurement of NP properties at these three sites is increasingly difficult, and the achievable accuracy and precision fall quickly with polydispersity, typical for aggregates and agglomerates.

Mathematical models are used to estimate these parameters, assuming that in in vitro models, particle delivery is driven by diffusion and sedimentation [121], regardless of whether the particle is stable or not [122]. The rate of diffusion and sedimentation of a particle are determined by the hydrodynamic radius and effective mass density, where the adsorption of proteins will alter both metrics. The rate of transport, and thus, the rate of particle delivery can be estimated via modelling, provided that these hydrodynamic properties are known [123–127].

The delivery profile of NPs is also determined by the ability of the cell to internalise the particles. From the point of view of the NP, uptake is dependent on size, shape, elasticity, and surface chemistry [126, 128–133]. Thus, the physicochemical characteristics of NPs in CCM strongly impacts their deposition and interactions on the outer cell membrane, as well as the potential induction of cellular responses [134]. From the point of view of the cell, the principal mechanisms whereby NPs interact and impact upon target cells occurs through their interaction with cell membranes, endo-lysosomal vesicles, nucleus and organelles [135–137]. Cell types also differ in lipid and receptor composition of the membrane, where modifications have been shown to alter the membrane fluidity and cellular functions and consequently NP uptake [138–140]. Additionally, NPs adhering to the outer cell membrane also can induce adverse responses [141], for instance, a pro-inflammatory response via oxidative means [142], the fibre paradigm [143] and genotoxicity [144]. The use of reliable methods and realistic test conditions to study possible effects of NPs on cells have recently been reviewed in several publications [145, 146] and are covered in the Chapter titled, “Molecular and Cellular Aspects and Methodological Approaches”.

The intracellular fate of NPs upon interaction with cells (uptake, retention, release, intracellular degradation, transfer to other cells, and/or translocation across tissue barriers) is still poorly understood but there seems to be an agreement that solubility, size and surface charge are the most important determinants of a material's fate in vitro as well as in vivo [147]. Therefore, it is imperative that the characterisation and understanding of NP in complex media is performed as accurately and realistically as possible in order to understand the physicochemical phenomena driving their interaction with cells.

5.6 Measuring NP in Complex Cell Culture Media: Different Methods, Pitfalls and New Developments

In this section, available methods for the characterisation of NP in complex media will be discussed. It is divided into four parts: **scattering**, **separation**, **imaging** and **dynamic** methods.

5.6.1 *Scattering and Spectroscopic Methods*

Light scattering instruments are well-established techniques for the characterisation of NP and consequently are the most frequently used to obtain information about the behaviour of NPs in complex media.

The average size (hydrodynamic diameter) of NPs can be characterised by dynamic light scattering (DLS), depolarized dynamic light scattering (DDLS), fluorescence correlation spectroscopy (FCS), small-angle neutron scattering (SANS),

small-angle X-ray scattering (SAXS), static light scattering (SLS), X-ray diffraction (XRD) and UV-Vis spectroscopy in case of plasmonic NPs. Characterizing polydispersity and size distribution is not as straightforward with FCS, XRD, and UV-Vis. DDLs is especially well-suited to studies in CCM when the NPs exhibit optical anisotropy, such as gold, silver, ZnO, TiO₂. In this case, the experimental accuracy benefits from the fact that the scattering of depolarized light from the CCMs is weak, and thus, an excellent ‘contrast’ in favour of the NPs can be obtained [115, 148]. Information about stability, protein adsorption, aggregation, integrity, such as dissolution and loss of ligands, can be obtained with techniques that are used to measure particle size.

Information about particle shape can be obtained via DLS, DDLs, SANS, SAXS, and SLS. Additionally, plasmonic and anisotropic NPs, such as metallic nanorods and nanostars, have unique signatures in the UV-Vis spectrum. For metallic NPs, the red shift of the plasmon resonance peak in the UV-Vis spectrum can either signal aggregation or the formation of a thick protein or polymer shell around the particle. In the case of particle agglomerates, the “fractal dimension” is a measure of the density of packing of the primary particles that could be redefined as the porosity of the aggregates. This information can be obtained with SLS, SAXS and SANS. Structural information about the protein corona beyond its thickness, (e.g. density as a function of distance from the particle surface), can also be obtained via SANS [148–151].

Another important aspect is that these techniques give a holistic representation of the sample; consequently, the protein-rich background signal must be very carefully and justly addressed. Figure 5.4 compares the dynamic light scattering analysis of silica particles in water to its scattering in complex CCM. While the particles are relatively large (100 nm in diameter) the CCM scatter nearly as much as the particles themselves, and therefore, strongly interfere with the signal (called the correlation function) to be analysed in order to characterise the NPs.

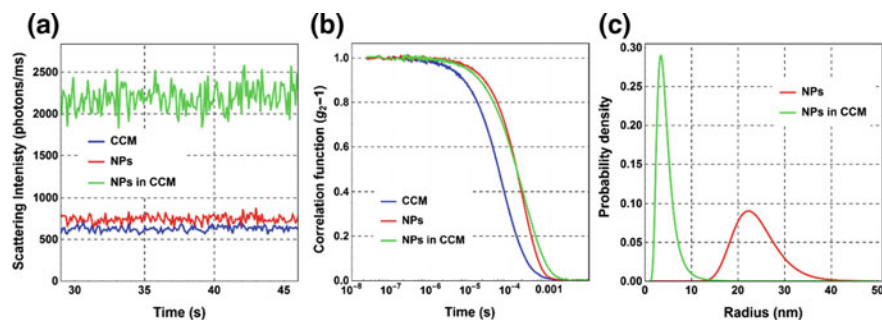


Fig. 5.4 a The intensity of light scattering from silica particles in water, from the CCM, and from the particles in CCM. (SiO₂ NPs, 100 nm, 20 μg/ml, scattering angle: 90°, CCM: RPMI suppl. with 10% foetal calf serum). b The corresponding signals to be analysed (correlation function). c Due to the strong scattering from proteins, the NPs in CCM appear to be smaller than in water

5.6.2 Zeta Potential—Describing the Surface Charge of NP

The surface charge of a particle is usually described by measuring the zeta potential, which is the electrokinetic potential at the slipping plane, not the true potential found at the particle surface itself (Fig. 5.5). Consider a negatively charged NP immersed into a complex media. Due to its charge, ions and molecules with the opposite charge form a strongly adhered layer (Stern layer) around the particle. Beyond the Stern layer, a loosely bound and mobile layer develops, comprised of both negative and positive charges. The edge of this layer is known as the slipping plane. When the particle moves, ions and molecules within this plane move along with the NP, but ions and molecules beyond the slipping plane do not, thus, it is at this point the zeta potential is measured. When NPs enter CCM, different proteins and other organic molecules can adhere to their surfaces. The properties of the corona highly depend on the surface characteristics and on the type of the CCM [90]. As can be seen, the zeta potential is exemplary case demonstrating that this physicochemical property of the NP cannot be decoupled from the context of its actual environment.

5.6.3 Measuring the Effect of Proteins on Zeta Potential

The understanding of the zeta potential of a particle is an important tool for understanding their long term colloidal stability and efficiency on surface functionalisation [152]. However, the zeta potential obtained for NP in CCM can be easily misinter-

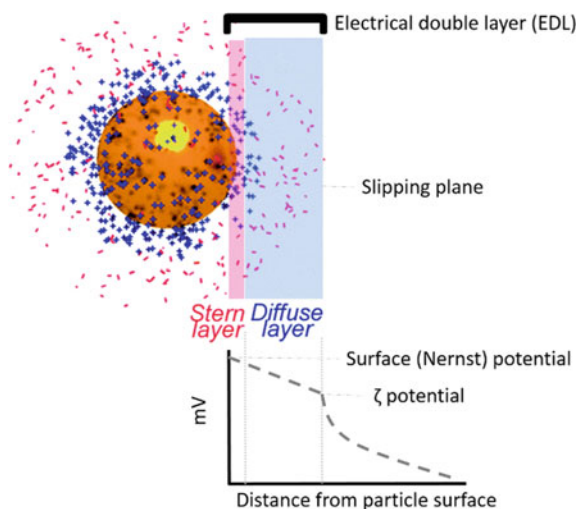


Fig. 5.5 The arrangement of ions surrounding a negatively charged particle. The important parts of the electrical double layer are highlighted. Adapted from [3]

preted. The ideal NP sample for zeta potential analysis using electrophoresis is as follows: (1) monodisperse in size and with high light scattering properties; (2) dispersed at low salt concentration (conductivities (Λ) < 1 mS/cm); and (3) dispersed in a particulate-free, polar dispersant (e.g. high purity water). Particles delivered in CCM clearly do not meet all of these criteria and thus, may not give high quality zeta potential data. Common challenges with this type of sample are:

- CCM contain high salt concentrations and as a consequence high sample conductivity (Λ is 1.5 S/cm) [153], which raises the likelihood of Joule heating (the process where the energy of an electric current is converted into heat as it flows through a resistance) and consequently lead to electrode polarisation and degradation due to the movement of the conductive ions.
- In many cases, NPs selected for biological applications usually have a diameter of < 20 nm, which have a high mobility in suspension due to the applied field and Brownian motion [154] and so have very low light scattering properties [155]. Therefore, the electrical field needs to be applied for long integration times to increase the signal-to-noise ratio. Consequently, Joule heating of the sample may also occur. Since the mobility is calculated directly from the sample viscosity, this temperature increase creates a substantial systematic uncertainty in the electrophoretic mobility measurement.
- Proteins can aggregate immediately at the electrodes even at extremely low voltages and due to the integration times required for weakly scattering NPs. These protein aggregates can migrate into the optical detection region of the cell, leading to measurement of the electrophoretic mobility of the aggregates, rather than that of the NPs [156].
- Zeta potential is only obtained by using mathematical models to extract it from the electrophoretic mobility of the particle. In general, a proportionality between electrophoretic mobility and zeta potential is assumed. While this proportionality is dependent on ionic strength, for high values of zeta potential, electrophoretic mobility can either be independent of zeta potential, or non-monotonic behaviours can occur, which limit the accuracy of the obtained zeta potential value.

Due to the aforementioned challenges, it is important to understand the strengths and limitations of zeta potential measurements of NPs in CCM when interpreting results. For this, a “special” sample preparation is recommended in order to improve data quality in terms of accuracy and reproducibility:

- The CCM should be filtered before adding to remove the possible protein aggregates and any visible particulates.
- The dilution of CCM to decrease the conductivity is a way to protect the electrode and typically improves data quality. It is important to re-measure the pH after dilution.
- The characterisation of hydrodynamic size of the NPs before and after measuring zeta potential can reveal any interaction between the sample and the electrode material (e.g. protein and formation of NP aggregates).

- Centrifuging the sample and reconstituting in “clean media” is a method of “washing” the NPs and reducing conductivity. It is worth noting that this procedure should not have an effect on the original colloidal stability and the original pH.

5.6.4 *Choosing Scattering Methods for Nanoparticles in Complex Media*

Nanoscience is intrinsically an interdisciplinary approach, therefore the range of skills and expertise within a research group are becoming more and more multidisciplinary. Probably the best thing that the typical researcher engaged in nanomedicine and nanotoxicology can do is to collaborate closely with instrument scientists having the necessary theoretical and experimental expertise in the techniques of choice. Basic guidelines that outline the function and utility of scattering techniques are summarised in Table 5.2.

5.6.5 *Characterisation Methods Based on Separation*

A different approach to extract information about NP is to separate them via external fields and use their response to the field to gain information about their size and size distribution. Three fields are commonly used for this purpose: centrifugal force, flow fields and electrical fields.

5.6.5.1 *Analytical Centrifugation*

Centrifugal force is used in analytical ultracentrifuge (AUC) and disc centrifuge (DC) analysis [176–180]. The principle of analytical ultracentrifugation is to expose NP to a very strong acceleration (up to a million times that of gravity). Under these conditions, particles and macromolecules experience an enhanced sedimentation velocity, which is proportional to their mass minus their buoyancy, and inversely proportional to their hydrodynamic radius. Therefore, any difference in either their mass or their hydrodynamic radius is enormously amplified in an ultracentrifuge. This permits the separation of particles with differences in mass, in density, or simply in their hydrodynamic radius. In its basic configuration, an analytical ultracentrifuge is coupled to a UV-Vis detector operating at single wavelength, or to a refractive index detector, which allows one the determination concentration of all particles passing through a detection window. Determining the concentration clearly requires the knowledge of the object shape, which defines the amount of light scattered and adsorbed by it. The most advanced versions of the analytical ultracentrifuge can measure full UV-spectra at multiple wavelengths all along the sample tube, thus providing sedimentation pro-

Table 5.2 Summary of the information that can be obtained from scattering, spectroscopic and separation based analysis techniques covered in Sect. 5.6

Technique	Properties of NPs the technique directly based on	Recommended usage	Warnings	Properties derived indirectly	Information deduced	Typical pitfalls and/or benefits	References
DLS	Optical polarisation Translational diffusion due to Brownian motion	Uniform NPs characterised in non-complex matrices, such as water	Presence of proteins may strongly scatter light, which interfere with the analysis, (Fig. 5.4) Polydispersity (apparent particle size may be defined by only a few large NPs)	Hydrodynamic radius	Particle size Polydispersity Colloidal stability Thickness of protein corona	Improper sample preparation/purification Isolation of 'protein signal' is erroneous or forgotten Converting particle size and polydispersity values into number-averaged size distribution is done incorrectly Solution is not dilute enough (multiple scattering, inter-particle interactions)	[157–160]
DLS-Zeta potential	Optical polarizability Electrophoretic mobility: translational motion of NPs in quasi-static electric field	Uniform NPs characterised in non-complex matrices, such as water	Presence of proteins with non-zero electrophoretic mobility may strongly interfere with the signal Polydispersity: surface charge may be curvature dependent [161] Irregular shape	Electric double layer (EDL) describing the interface between NP and solution (solvent)	Potential difference between the slipping plane and solution Predict colloidal stability	Using wrong mathematical model for the type of media (e.g. the limiting cases of Hückel vs. Smoluchowski approximation)	[152]

(continued)

Table 5.2 (continued)

Technique	Properties of NPs the technique directly based on	Recommended usage	Warnings	Properties derived indirectly	Information deduced	Typical pitfalls and/or benefits	References
DDLS	Anisotropic optical polarizability Translational and rotational diffusion due Brownian motion	Both without and in the presence of CCM Uniform and optically anisotropic NPs (gold, silver, nanorods, tubes)	Compared to DLS, roughly three-times more sensitive to polydispersity of non-spherical particles	Hydrodynamic radius	Particle size Polydispersity Colloidal stability Thickness of protein corona	Improper sample preparation/purification Converting particle size and polydispersity values into number-averaged size distribution is done incorrectly Solution is not dilute enough (multiple scattering, inter-particle interactions)	[115, 148, 162–164]
FCS	Fluorescence Translational diffusion due to Brownian motion	Fluorescent labels may provide a high degree of selectivity towards the NPs	Polydispersity [165]	Hydrodynamic radius	Particle size	Stability and integrity of fluorophores Irregular shape and size polydispersity limits the accuracy of models available	[166–168]
SANS	The strength of interaction of neutrons with the atomic nuclei	Soft (light elements) NP Characterising the thickness and density of soft corona (proteins, polymers) around particles [151, 169] Magnetic NP Self-assembly	Presence of proteins in CCM may interfere with the analysis	Particle size and distribution Thickness and density of protein corona Functional layer, polymer coat Superstructure from particle Self-assembly	Particle size Polydispersity Particle shape and morphology (shell vs. sphere) Protein/Polymers corona	Analysis can be model-independent and model based Irregular shape and size polydispersity limits the accuracy of models available	[149, 150]

(continued)

Table 5.2 (continued)

Technique	Properties of NPs the technique directly based on	Recommended usage	Warnings	Properties derived indirectly	Information deduced	Typical pitfalls and/or benefits	References
SAXS	Electron density (number of electrons in each element's electron shells)	Both soft and inorganic NPs Self-assembly	Presence of proteins in CCM may interfere with the analysis	Particle size and its distribution Superstructure from particle self-assembly	Particle size Polydispersity Particle shape and morphology (shell vs. sphere)	Analysis can be both model-independent and model based Irregular shape and size polydispersity limits the accuracy of models available Insufficient information about biological surrounding of the NP	[150, 170, 171]
SLS	Optical polarizability	Both soft and inorganic NPs Self-assembly	Presence of proteins in CCM may interfere with the analysis	Particle size and shape Polydispersity	Particle size Polydispersity Particle shape and morphology (shell vs. sphere)	Analysis can be both model-independent and model based Irregular shape and size polydispersity limits the accuracy of models available	[17]
XRD	Electron density (number of electrons in the electron shells of each element)	Crystalline structure		Crystallinity Crystal structure	Crystallinity Average crystal line size Average particle size	Irregular shape and size polydispersity limits the accuracy of models available Little sensitivity to polydispersity Insufficient information about biological surrounding of the NP	[172]

(continued)

Table 5.2 (continued)

Technique	Properties of NPs the technique directly based on	Recommended usage	Warnings	Properties derived indirectly	Information deduced	Typical pitfalls and/or benefits	References
TDA	Optical extinction. Brownian motion. Dispersion in laminar flow	Poorly purified samples Ultra-small NPs Multimodal suspensions	Hydrodynamic radius Poor time resolution (kinetics)	Particle size Polydispersity	Particle size Polydispersity	Irregular shape and size polydispersity limits the accuracy of models available Microfluidic environment is needed	[173, 174]
UV-Vis	Optical extinction	NPs exhibiting plasmon resonance	In case of protein corona/polymer shell, aggregation is not indicated	Particle size Polydispersity	Average size Concentration	Little sensitivity of analysis to polydispersity	[175]
AUC/DC	Sedimentation velocity, optical extinction	Possibility to resolve the particle size distribution and multimodality Distinguish between different materials	Loosely bound proteins and macromolecules can be detached	Hydrodynamic radius, full characterisation of the size distribution	Separation of particles by population, including clusters	Irregular shape of particles requires advanced modelling	[176–180]
AFFF	Diffusion coefficient	Separation of particles based on size, and their independent characterisation	Loosely bound proteins and macromolecules can be detached. Interaction with membrane might be troublesome	Particle hydrodynamic radius, particle shape (via SLS)	Separation of particles by population, including clusters	Irregular particle shape; interactions with membrane is particle dependent	[79, 181]
TRPS	Particle volume and electrophoretic mobility	Individual particle counting and size/electrophoretic mobility measurement	High ionic strengths are required to measure small particles	Particle volume	Size distribution Zeta potential distribution	Particle colloidal stability Aggregates might cause blockage of the pore	[182–184]

files with full UV-Vis characterisation of the centrifugate [177, 179]. This method has been used to characterise gold NP undergoing aggregation, as well as mixtures of quantum dots.

Disc centrifugation is a cheaper and simpler variation of ultracentrifuge, operating at a much lower number of revolutions per minute, where particles are injected in proximity to the centre of a spinning disk, and a single wavelength detector is used to measure their concentrations at a given passage point [180]. While unable to provide the same amount of information as ultracentrifuge, this technique is highly versatile, and suitable for separation and characterisation of NP covering a broad range of sizes, especially high density inorganic NP. One particularly interesting feature of centrifugation-based characterisation methods is the possibility to separate NP from clusters with two, three, four particles, thus allowing a much more precise assessment of the cluster mass distribution in the case of aggregation. This is one of major advantages compared to scattering techniques, which probe solutions without any separation of the different components.

The disadvantages of centrifugation techniques are that: (1) they usually require dilution of the sample, which could change the quantity and composition of proteins and ions adsorbed on their surface, and (2) quantitative interpretation of the data is only possible when the shape of the particles and clusters is known, which determines their hydrodynamic radius. Except for very simple shapes, the determination of hydrodynamic radius is usually a complicated problem, and irregular particles are characterised by sedimentation velocity that are a function of their orientation.

5.6.5.2 Taylor Dispersion Analysis (TDA)

Taylor dispersion analysis is another method that can be used to determine the size and size distribution of particles [173, 174]. The principle is based on the injection of concentration pulse of particles in an empty capillary, where a parabolic flow profile leads to a dispersion of the particles. Because particles close to the middle of the channel travel faster than those close to the walls, a concentration gradient in the radial direction is created. This concentration gradient is compensated by particles diffusion, which tends to create a uniform concentrations profile in the radial direction. Therefore, a measurement of concentration at two different positions along the channel allow one the determination of the particle diffusion coefficient and its distribution, from which size is extracted. While the technique has been widely used to determine the molecular weight of biological macromolecules, the application to particles is only recent. Some configurations exist, where Taylor dispersion has been used in combination with capillary electrophoresis, which can be used to speed up the analysis. The method represents a reliable alternative to DLS in the determination of particles diffusion coefficient, because it requires a much simpler setup, but suffers from the usual limitations of how to relate the diffusion coefficient to particle shape. In addition, since particles are exposed to a shear rate, adsorption of molecules on their surface could be affected by the flow field. Furthermore, compared to the analytical centrifugation method, TDA cannot fractionate the samples, thus is less accurate in

determining the particle size distribution, even though a recently introduced moment-based method to obtain more accurate size information has been proposed [173, 185, 186].

5.6.5.3 Asymmetric Flow Field-Flow Fractionation (AFFF)

This technique is able to fractionate a sample by exposing it a laminar flow field and perpendicular cross-flow in order to determine particle size distribution in biologically-relevant samples [181]. A small sample of particles in solution is injected in a channel with a laminar parabolic profile. Perpendicularly to the flow direction, another flow field is applied. As a result, large particles tend to be driven towards the bottom part of the channel, while smaller ones, having larger diffusion coefficients, stay closer to the centre of the channel. Large particles take longer times to flow through the channel than smaller ones. The perpendicular cross flow is obtained by removing part of the main flow in the channel through a membrane positioned on one of the sides of the channel. The cut-off of the membrane determines the minimum size of particles or macromolecules that can be detected. AFFF can be used to separate particles from clusters, to determine the size of particles, including the presence of a coating on the particles. Quite often, is AFFF coupled to detectors, such as DLS and multi-angle light scattering, in addition to more common refractive index detectors, used in chromatographic processes. While in the oldest versions of the methods a calibration of the elution time was necessary to determine the size of the eluting particles, similar to what used in gel permeation chromatography, the use of modern detectors allows one to measure the absolute values of the size of the particles that elute, and also to obtain information about their shape. The elution time of the particles can be further controlled by tuning the flowrate and the extent of crossflow. Therefore, the combination of the fractionation ability of the AFFF with the presence of these advanced detectors, make this method one of the most versatile and powerful in the characterisation of particles.

However, the method has also some limitations. The exposure of particles to shear forces, as well as the intrinsic dilution that the particles are subject to, can easily lead to desorption of proteins from particles exposed to complex media. This has been exploited to distinguish between strongly bound proteins versus weakly bound proteins, which have been both detected separately [79, 178]. In addition, the interaction of particles with the membrane in the channel is one of the major concerns of the AFFF. Depending on the material of the membrane, particles can be repelled, or can adhere to the membrane, thus resulting in partial loss of analyte, and difficulty in assessing whether the analysis of the sample is thorough.

5.6.5.4 Tuneable Resistive Pulse Sensing (TRPS)

A completely different approach is the one used by Tuneable Resistive Pulse Sensing (TRPS) [182]. In this case, particles immersed in an electrolyte solution are exposed

to an electric field and forced to move through a narrow pore. The measurements are done at such a low concentration that only one particle at a time passes through the pore. The presence of electrolytes in the solution leads to a steady passage of electrical current through the pore. However, as one particle passes through the pore, a drop in the electrical current ensues, which is proportional to the volume of the particle. Additionally, the shape of the resistance pulse depends on the electrophoretic mobility (and zeta potential) of the particles. This technique enables not only a precise determination of the particle size, provided that the particles are stable under electrolyte conditions used during the measurement, but also the assessment of the particle concentration. Interestingly, the size determination is independent of particle shape and material. Because the method is based on counting individual particles, an accurate determination of size distribution, even in the case of multimodal distribution of particles, is possible.

The technique can also create maps of particles based on not only their size, but their zeta potential too [183, 184]. This opportunity has been used to characterise particles with a protein corona obtained by exposing them to bovine serum, and the results have been compared to those obtained by DLS and by analytical centrifugation. The main drawbacks of TRPS are the following: (1) particles with a size lower than 30 nm cannot be detected, and, additionally, (2) small sized particles require high electrolyte concentrations, which might hamper their colloidal stability. Additionally, pore size must be not much larger than the particles, otherwise the limits of detection will be hit, and the presence of clusters of particles will result in blocking of the pore.

5.6.6 *Microscopic Methods*

5.6.6.1 **Advancements in Light Microscopy (LM)**

The theoretical resolution limit of light (~200 nm) defines the size limit of objects that can be resolved by standard light microscopic methods. The resolution limit can be improved by capturing the absorption/scattering of light by an object in a Fourier plane by the objective lens and converted into a real plane image by the ocular lens, thereby providing additional resolution on nanostructures in a technique called Fourier plane imaging [187]. This requires the use of a rotating grating to obtain inaccessible high-resolution information that are encoded into the Fourier plane. Combining these images in the Fourier space yields information that is converted into a higher resolution of the (real) image [188] and is applicable to a biological complex setting [189]. Such computational approaches push the 200 nm size limit of a standard light microscope to somewhere around 50–100 nm.

Besides computational advancements, additional hardware can provide improvement in resolution. The detection of strongly scattering NPs, such as gold NP and multiwall carbon nanotubes, profits from cardioid condensers provided in enhanced darkfield microscopic imaging [190]. The oblique illumination reaches a resolution

around 90 nm and accentuates the effects of strongly scattering particles and reduces the contribution of the much less strongly light scattering complex environment [191, 192]. With this method, it is also possible to determine the aggregation state of the particles.

If the information on the absorbance and/or reflection of the incoming electromagnetic wave is insufficient, one must rely on a signal inherent and exclusive to the NP. In the case of superparamagnetic iron NP (SPIONs), the inherent ability to convert electromagnetic energy into heat can be exploited for their detection. Hence the usage of such particles in clinical settings as contrast enhancers in magnetic resonance imaging. More recently, lock in thermography (LIT) uses this ability to study the heating power of clinical applications of SPIONs [193].

The bioimaging of NPs rely on an exclusive light signal originating from the particles, typically achieved by covalent bonds with fluorescent dyes [194, 195]. Unfortunately, these approaches are of limited interest to natural NP in complex media since NP in consumer products are seldom tagged with such fluorescent dyes.

5.6.6.2 X-Ray Microscopy

Owing to the smaller wavelength of X-rays, X-ray microscopy (XRM) resolves objects up to a spatial resolution of about 30 nm without the need for a vacuum (as in electron microscopy, see below) [196]. Scanning transmission X-ray microscopy (STXM) has been used, for example, to monitor copper NP in river biofilms [197].

5.6.6.3 Scanning Probe Microscopy

Scanning probe microscopy, especially atomic force microscopy (AFM), is an often-used method to measure NP. AFM provides a three-dimensional surface profile by raster-scanning a sharp tip (few nm to 10s of nm) over a surface with a feedback loop to adjust parameters needed to image a surface. Atomic forces are used to map the tip-sample interaction and can be used for all types of nanomaterials.

Most AFMs use a laser beam deflection system where a laser beam is focused on the back of the reflective AFM lever onto a position-sensitive detector. The acquired height map can provide the height of NP with unprecedented accuracy and precision. Although AFM can operate both in air and in solution, the former procedure is much more present in literature owing to an easier procedure [198].

5.6.6.4 Electron Microscopy

The wavelength of electrons in an electron microscope is another 1000 fold smaller than the wavelength of X-rays in XRM and 10,000 fold smaller than photons in optical light microscopy. Therefore, electrons can convey much smaller information providing sub-Ångstrom resolution. Two types of electron microscopy are commonly

utilised: scanning electron microscopy (SEM) and transmission electron microscopy (TEM).

A scanning electron microscope operates by registering the interaction between the sample and a focused electron beam that scans over the sample. Dedicated detectors can collect back scattered electrons and secondary electrons. Backscattered electrons (BSE) are electrons provided by the focused electron beam that are slingshot back under the influence of positively charged atomic nuclei. The BSE yield relates to the proton density: the heavier the atoms the brighter BSE the signal [199]. This relationship can be used to differentiate between two components, e.g. a metal NP in a carbon-based medium. Secondary electrons (SE) are electrons that derive from the inelastic collision of the electron beam with the electron shell. They originate from the atoms within the samples and will result in ionisation events. SEs mainly contain topographic information on the surface of the object. SEM provides a unique view on the surface of particles and allows for size estimation, surface structural analysis and surface defects detection for particles of a few nm diameter or higher.

In a TEM, the shadow of the object, as witnessed by the electron beam, is imaged. TEM provides the highest resolution of all known microscopic methods: around 0.2 nm in conventional instruments and even 0.05 nm in high-end aberration corrected instruments [200]. Darkfield approaches, similar to in light microscopy, such as scanning transmission electron microscope (STEM) and variants such as high-angle annular darkfield provide high contrast in function of the atomic number thereby permitting differentiation between the signal of non-carbon-based NPs and the typically carbon-based medium in the image [201].

Electrons have a much stronger interaction with matter than the other electromagnetic waves described above. Consequently, electron microscopes must operate under a vacuum as electrons will be scattered by the atmosphere. However, water will evaporate at room temperature in the vacuum of an EM. This implies that aqueous samples require complete dehydration prior to measuring [202]. If removing the aqueous medium is not an option, for example because it is an integral structural component as in liposomal preparations, cryo-electron microscopy can be useful. Water in frozen samples will remain in its solid form at liquid nitrogen temperatures, even at the low pressures inside the electron microscope. Cryo-EM has the additional advantage that drying-induced aggregation or structural changes are prevented. Such low temperature approaches are possible both in SEM, TEM and STEM.

Another possibility to image without removing the aqueous solution is to sacrifice resolution for the presence of water in the sample, a concept which is applied in the environmental scanning electron microscope (ESEM). Differential pumping permits to have the electron optics under high vacuum but the sample chamber under a poorer vacuum: typically around 50–100 mbar, 1/20 of the ambient pressure. A 10-fold reduction in resolution compared to conventional SEM is the main drawback (in the range of 50–100 nm), along with a very limited penetration depth of the beam. Efforts were made to develop sample chambers, WetSEM™ capsules, which enclose the sample including the liquid environment inside the vacuum of the electron microscope. These capsules are equipped with an electron-transparent membrane that allows electrons to pass into the sample. More recently, liquid TEM holders have

been developed, based on a similar principle of shielding the aqueous samples from the vacuum in the instrument by means of silicon nitride windows [203].

5.6.6.5 Analytical Methods

The microscopic approaches discussed above result in images that reflect the absorption, reflection and/or scattering of the incoming electromagnetic waves. Most imaging modalities can be complimented with analytical tools, often of spectroscopic nature. These analytical tools provide a means to characterise the wavelengths present in the image-forming waves, i.e. the spectral fingerprint. The analytical microscopy concept turns the 2D micrographs into 3D data cubes, with the third dimension a spectrum for each pixel that can be matched with existing libraries.

Light microscopic methods can be complemented with visual and infrared range spectroscopy (400–1000 nm). Such spectroscopic analyses have been used in combination with dark field microscopy to study the interaction between cells and NP in the absence of a fluorescent probe [204], where the spectrum can be influenced by the surrounding matrix [205]. Other spectroscopic possibilities, such as Raman spectroscopy or Fourier transformed infrared spectroscopy can be used.

The interaction of an electron beam with the inner shell electrons of atoms can result in the expulsion of X-rays which are characteristic of the atom. The specific X-ray energy can be detected and quantified by a silicon drift detector, an analytical method known as electron dispersive X-ray or EDS. EDS provides the chemical characterisation for each pixel in the image, resulting in elemental maps, and can be found in SEM and STEM setups. A second spectroscopic method in found TEM and STEM based on electron interactions with atoms is called electron energy loss spectroscopy (EELS). Electrons in a high voltage, coherent electron beam hitting outer shell electrons of atoms will lose energy by inelastically scattering electrons in a way that is characteristic for the interacting atom. Peaks in the absence of a specific energy band quantify elements in the sample [206].

5.6.6.6 Advice for Sample Preparation for Imaging Techniques

Unlike scattering methods, microscopy provides results on a per particle basis. This necessitates the creation of proper sampling schemes: each nano-object must have the same chance to be sampled, independent of its size or other characteristics. Omission bias (larger objects are favoured) or convenience sampling (searching for a convenient example) render data unsuitable for generalisation and hence useless to represent the entire nanomaterial. The key to overcome such bias is to record data according to a (computer-) generated randomised scheme [207]. A summary of the discussed techniques can be found in Table 5.3.

Table 5.3 Summary of imaging techniques used in the elucidation of colloidal interactions at the bio-nano interface

Technique	Information	Pro	Cons	Pitfalls
Structured illumination microscopy	Presence of NP	Sub 100 nm resolution	Will not resolve NP	Processing time. Artefacts due poor grating position
Darkfield microscopy imaging	Presence and localization (unresolved) of NP	Light microscopy based, easy sample prep	Only strongly scattering NP	Interpretation of the data can be arduous
Fluorescence microscopy (including laser scanning microscopy and super resolution microscopy (STED, PALM, STORM))	Presence and localisation (unresolved) of NP	Light microscopy based, easy sample prep. <100 nm resolution in super resolution LM	Necessity for fluorescent dyes	Fluorescent staining of NP in complex media can be difficult
Magnetic resonance imaging	Presence and (crude) localisation of NP	Non-invasive, and very specific	Poor resolution, limited to paramagnetic NP	
Lock in thermography	Presence and thermal signature of paramagnetic and plasmonic NP	Sensitive, reliable	Poor resolution, limited to paramagnetic particles	
Atomic force microscopy	Presence, localisation, size	High resolution, in aqueous solutions	Bias in height values due to deformation by the cantilever tip [138]	User influence on the data processing [139]
XRM XRSM	Presence, aggregation, size distribution	No sample prep needed	Synchrotron or advanced light source needed	
Scanning electron microscopy	Presence, aggregation, size distribution, surface analysis, surface defects detection, material contrast information	Resolves single particles, high resolution, Bulk samples	Vacuum needed, meaning drying of the particles, may induce aggregation. Samples may need conductive coating, destructive method (samples cannot be reused)	Size estimation can be complex for non-spherical NPs
Environmental scanning electron microscopy	Presence, aggregation and size of (larger) NP	In situ electron microscopy	Loss of resolution	Complex image interpretation

(continued)

Table 5.3 (continued)

Technique	Information	Pro	Cons	Pitfalls
Transmission electron microscopy	Presence, aggregation, size, morphology, 3D structure	High resolution	Sample preparation: water must be removed	Only thin objects (<200 nm thick)
Scanning transmission electron microscopy	Presence, aggregation, size, morphology, 3D structure	High resolution, thicker samples (up to 1 μm)	Sample preparation: water must be removed	Radiation damage of the sample
wetSEM	Presence, aggregation state, size, morphology	Electron microscopy without the need for dehydration	Loss of resolution	Sensitivity of the membrane to radiation damage
Liquid holders TEM	Presence, aggregation state, size, morphology, 3D structure	Electron microscopy without the need for dehydration	Dedicated chips needed for each sample	Interaction of electron beam on enclosed water complicates interpretation

5.6.7 Dynamic Methods

The interactions of NPs *in vivo* have been shown to be a dynamic affair, where the faster moving proteins arrive first, forming the ‘soft corona’, and then are replaced by less motile proteins that have a higher affinity for the surface and become electrostatically bound, forming the ‘hard corona’, over the course of several hours [208–210]. Full understanding of any dynamic behaviour necessitates its study in space and

Table 5.4 Summary of dynamic techniques

Technique	Information	Pros	Cons	Pitfalls
Synchrotron techniques	NP properties, chemical composition and protein aggregation	High flux allows for excellent resolution in space and time	Samples are easily damaged by synchrotron radiation Beamtime is not easily awarded	Data deconvolution can be complex
Microfluidics	Interfacial phenomena	Can be coupled with scattering and imaging techniques Can overcome sample preparation issues found in bulk	Interdisciplinary knowledge of optics, and fluid mechanics in addition to your own expertise are required	Devices are not ‘plug and play’ units Resolution is limited to the detection method Detection methods are limited by chip material

in time. As the interaction of NPs with components in physiological media is a dynamic phenomenon, scientists are utilising advanced, high energy synchrotron techniques, coupling microfluidic technologies with scattering or imaging methods, and/or sophisticated software to analyse images in order to obtain time resolved data (Table 5.4).

5.6.7.1 Synchrotron radiation

The brilliance of synchrotron radiation has significantly shortened the analysis time of a multitude of scattering techniques in specialised facilities that can be found around the world. Synchrotron light is produced by the acceleration of electrons under the direction of a magnetic field to 99.9% of the speed of light. This results in the production of radiation that has high flux, a wide energy spectrum, highly collimated and polarised, which can produce short pulses. Such radiation allows for the fast illumination of NP at the bio-nano interface, where data deconvolution allows for the separation of signal between the protein and NP. Because of the advantages of high spatial resolution, high sensitivity, excellent accuracy, low matrix effects and non-destructiveness, synchrotron radiation analytical techniques are increasingly becoming valuable tools for investigating the bio-nano interface.

By selecting and directing specific wavelengths of light to specific instruments, called ‘beamlines’, one can utilise specific wavelengths of radiation, to analyse the bio-nano interface within one facility. Of particular utility for the dynamic analysis of NP in complex media are the following methods.

Synchrotron Small Angle X-Ray Scattering (SAXS)

High brilliance synchrotron sources coupled with advanced detectors has ensued the adoption of time resolved synchrotron SAXS data to observe a multitude of dynamic processes, thus helping us to understand the link between nanostructure and the properties of the materials [211]. Synchrotron SAXS, coupled with SANS, has been used to observe changes in morphology of gold NP upon interaction with physiological proteins [150]. This detailed study employed complex data deconvolution in order to elucidate protein dissociation constants, and the stoichiometry of the NP-protein complex, where the authors developed their custom built software in order to make this technique accessible to non-experts in small angle scattering. In a more straightforward manner, highly ordered nanomaterials can particularly benefit from dynamic study with synchrotron SAXS, where changes in scattering are more evident. This method has been used in the determination of the kinetics of disorder-order and order-order phase transitions in lipidic liquid crystalline NP, upon exposure to lipases [212, 213].

Synchrotron X-Ray Absorption Spectroscopy (XAS)

X-ray absorption spectroscopy detects change in the local electronic environment, coordination geometry and bond distances of absorbed atoms in materials [214]. Because of its unique chemical sensitivity, synchrotron XAS provides precise fingerprint measurements of the NP structure, shedding light on the molecular mechanism of physicochemical interactions, such as adsorption, dissolution, phase transformation, and oxidative-reductive reactions, at the interface between NP and physiological milieu [215]. Additionally, synchrotron X-ray sources can be focused to spot sizes ranging from mm² down to the nm² range [216]. XAS reveals specific information of specific sites in three different energy regions: the pre-edge region, which reflects electronic structure and oxidation state; the X-ray absorption near edge structure (XANES) and the extended X-ray absorption fine structure (EXAFS), providing geometry and coordination of the local structure. An important advantage of XAS is that samples of all states of matter (gas, liquid, soft matter and solid) can be analysed.

For instance, XANES has been used to differentiate the chemical states of iron on the surface of two types of Fe₂O₃ NPs (α -Fe₂O₃ and γ -Fe₂O₃) in the presence of biological reducing agents cysteine and NADPH [217]. Binding sites of BSA upon gold nanorods have also been identified via XANES in combination with a least squares linear fitting [218]. XANES experimental data combined with simulations revealed that the hydrophobic interaction between a streptavidin and the hydrophobic surface of single-walled carbon nanotubes induced changes in the C=O double bond of the streptavidin which subsequently led to a small, but relevant structural distortion of the protein [219]. As can be seen, XAS is a powerful tool for characterizing the chemical states of NP and proteins at the interface between NP and biological milieu.

Synchrotron Circular Dichroism (CD)

The main advantage of synchrotron CD over benchtop instruments is that it has the capacity to obtain structural information of proteins with only small sample amounts in a short amount of time. By following the unfolding of different classes of human plasma proteins upon exposure to gold and silver NP at different temperatures, Laera et al. demonstrated that albumin, transthyretin and lysozyme are significantly destabilised when interacting with silver NP, whilst its stability is not affected when interacting with gold NP [110]. Time resolved synchrotron CD has been utilised to observe rapid changes in the folding of BSA in the corona, attributed to the transformation of protein disulfide bonds to Au-S coordination [218]. Thus, the rapid acquisition of CD data can be used to reveal the molecular mechanisms of interfacial reactions of proteins.

Advances in Synchrotron Techniques

Recent developments in synchrotron instrumentation have afforded scientists the ability to visualise NP on a single particle level. Coherent X-ray diffraction is a powerful method of measuring the three dimensional structure of NP, where 2D or 3D reconstruction of the scattering pattern allows for the elucidation of an image of nanoscale structures [220]. The most recent advances in this field have been in X-ray free-electron lasers, where femtosecond flashes of X-ray light have been used to provide single particle analysis on nanoscale particles, in this case, a crystalline gold core and a differently shaped palladium shell to a resolution of 7 nm [221]. These advances in synchrotron science will allow for a faster and more focussed understanding of interaction at the bio-nano interface.

5.6.7.2 Microfluidics

Microfluidics has facilitated the development of nanomaterials through the ability to accurately manipulate nanolitre volumes in microscale fluidic channels in turbulence free conditions, resulting in well-defined and well-controlled fluid-fluid interfaces to be made and manipulated [222]. Without agitation or obstacles within the channels, interaction between these interfaces at microfluidic length scales results only in diffusion controlled mixing. Microfluidic devices have thus been used in the creation of nanoscale materials, as fine control of the interfaces can be achieved through the directed introduction of valves, mixers and pumps on the chip in order to form uniform droplets and precipitates, and consequently, the precise control of NP synthesis [223] and separation [224]. In terms of looking at bio-nano interactions, chips can be designed and created in order to accurately mimic in vivo environments and processes, where the flexible and modular nature of microfluidic devices provides opportunities to create increasingly realistic models, including multi-tissue devices, which have been used to assess NP as drug delivery vehicles [225, 226].

Microfluidic chips can be combined with either scattering or optical techniques in order to understand how engineered particles behave in complex environments. Investigating NP dispersions under microfluidic laminar flow conditions coupled with fluorescence spectroscopy has previously been established as a technique known as flow cytometry [227], however the use of MF chips allows for this investigation in a more complex manner. The integration of sample preparation and delivery with the analytical mechanism results in the synergistic enhancement of function and performance of extremely small detection volumes (femtolitres to nanolitres). In order to monitor intra- and intermolecular reactions occurring in microfluidic reactors, they have been coupled with spectroscopic methods [228], surface-enhanced Raman spectroscopy (SERS) detection [229], Förster resonance energy transfer (FRET) [230], light scattering [231] and small angle x-ray scattering [232]. Thus, the flexibility of microfluidic chips allows them to be coupled to a wide range of characterisation techniques for the dynamic characterisation of NP at the bio-nano interface.

5.7 Conclusions and Future Directions

This chapter has:

- demonstrated that physiological fluids contain elements that alter the stability of NPs in in vivo conditions and that complex CCM have been formulated to reflect these conditions;
- demonstrated that colloidal chemistry phenomena of NPs are altered by elements in complex CCM;
- highlighted analytical techniques that are particularly useful to look at NPs in complex CCM; uncertainty surrounding colloidal interactions requires investigation by multiple techniques in order to get the complete picture;
- provided practical advice as to how these techniques need to be modified in order to take into consideration the effect of naturally occurring salts, surfactants and proteins upon the colloidal stability of NP in vivo;
- given insight into developing techniques that can be used to characterise the chemical and structural changes of the components at bio-nano interface;

In this way, a solid foundation for the long-term advancement of nanotechnology into effective new products both in medicine and industry can be established.

Acknowledgements This work was supported by the Swiss National Science Foundation through the National Center of Competence in Research Bio-Inspired Materials (WKF through the Research Program for Women in Science). The authors acknowledge financial support of the Swiss National Science Foundation (ML through grant number PP00P2_159258, BRR through grant number 310030_159847/1), the Adolphe Merkle Foundation, and the University of Fribourg. LRL acknowledges financial support from the Marie Curie COFUND Action (600375. NanoTRAINforGrowth).

References

1. Kim, B.Y.S., Rutka, J.T., Chan, W.C.W.: Nanomedicine. *New Engl. J. Med.* **363**(25), 2434–2443 (2010)
2. Bobo, D., Robinson, K.J., Islam, J., Thurecht, K.J., Corrie, S.R.: Nanoparticle-based medicines: a review of FDA-approved materials and clinical trials to date. *Pharm. Res.* **33**(10), 2373–2387 (2016)
3. Moore, T.L., Rodriguez-Lorenzo, L., Hirsch, V., Balog, S., Urban, D., Jud, C., Rothen-Rutishauser, B., Lattuada, M., Petri-Fink, A.: Nanoparticle colloidal stability in cell culture media and impact on cellular interactions. *Chem. Soc. Rev.* **44**(17), 6287–6305 (2015)
4. Guyton, A.C., Hall, J.E.: *Textbook of Medical Physiology*, 11th ed, p XXXV, 1116 p. Elsevier/Saunders, Philadelphia [etc.] (2006)
5. Yao, T., Asayama, Y.: Animal-cell culture media: history, characteristics, and current issues. *Reprod. Med. Biol.* **16**(2), 99–117 (2017)
6. Carrel, A.: On the permanent life of tissues outside of the organism. *J. Exp. Med.* **15**(5), 516–528 (1912)
7. Ebeling, A.H.: A ten year old strain of fibroblasts. *J. Exp. Med.* **35**(6), 755–759 (1922)
8. Fischer, A., Astrup, T., Ehrensvar, G., Oehlenschläger, V.: Growth of animal tissue cells in artificial media. *Exp. Biol. Med.* **67**(1), 40–46 (1948)

9. Zheng, X., Baker, H., Hancock, W.S., Fawaz, F., McCaman, M., Pungor, E.: Proteomic analysis for the assessment of different lots of fetal bovine serum as a raw material for cell culture. Part IV. Application of proteomics to the manufacture of biological drugs. *Biotechnol. Progr.* **22**(5), 1294–1300 (2006)
10. Eagle, H., Buffer combinations for mammalian cell culture. **174**, 500–503 (1971)
11. Stopford, W., Turner, J., Cappellini, D., Brock, T.: Bioaccessibility testing of cobalt compounds. *J. Environ. Monit.* **5**(4), 675–680 (2003)
12. Pagana, K.D., Pagana, T.J.: *Mosby's Manual of Diagnostic and Laboratory Tests*, 5th ed, pp. 1180. Elsevier Mosby, St. Louis, Missouri (2014)
13. Anderson, N.L., Anderson, N.G.: The human plasma proteome: history, character, and diagnostic prospects. *Mol. Cell. Proteomics* **1**(11), 845–867 (2002)
14. Hellstrand, E., Lynch, I., Andersson, A., Drakenberg, T., Dahlbäck, B., Dawson, K.A., Linse, S., Cedervall, T.: Complete high-density lipoproteins in nanoparticle corona. *FEBS J.* **276**(12), 3372–3381 (2009)
15. Kellum, J.A.: Determinants of blood pH in health and disease. *Crit. Care* **4**(1), 6 (2000)
16. Caracciolo, G., Farokhzad, O.C., Mahmoudi, M.: Biological identity of nanoparticles in vivo: clinical implications of the protein corona. *Trends Biotechnol.* **35**(3), 257–264
17. Choi, M.-R., Bardhan, R., Stanton-Maxey, K.J., Badve, S., Nakshatri, H., Stantz, K.M., Cao, N., Halas, N.J., Clare, S.E.: Delivery of nanoparticles to brain metastases of breast cancer using a cellular Trojan horse. *Cancer Nanotechnol.* **3**(1–6), 47–54 (2012)
18. Anselmo, A.C., Kumar, S., Gupta, V., Pearce, A.M., Ragusa, A., Muzykantov, V., Mitragotri, S.: Exploiting shape, cellular-hitchhiking and antibodies to target nanoparticles to lung endothelium: synergy between physical, chemical and biological approaches. *Biomaterials* **68**, 1–8 (2015)
19. Wick, P., Manser, P., Limbach, L.K., Dettlaff-Weglikowska, U., Krumeich, F., Roth, S., Stark, W.J., Bruinink, A.: The degree and kind of agglomeration affect carbon nanotube cytotoxicity. *Toxicol. Lett.* **168**(2), 121–131 (2007)
20. Teeguarden, J.G., Hinderliter, P.M., Orr, G., Thrall, B.D., Pounds, J.G.: Particokinetics in vitro: dosimetry considerations for in vitro nanoparticle toxicity assessments. *Toxicol. Sci.* **95**(2), 300–312 (2007)
21. Albanese, A., Chan, W.C.W.: Effect of gold nanoparticle aggregation on cell uptake and toxicity. *ACS Nano* **5**(7), 5478–5489 (2011)
22. Singh, A.K.: Physicochemical, electronic, and mechanical properties of nanoparticles. *Engineered Nanoparticles*, pp. 77–123. Academic Press, Boston (2016)
23. Zhang, Z., Wu, Y.: Investigation of the NaBH₄-induced aggregation of Au nanoparticles. *Langmuir* **26**(12), 9214–9223 (2010)
24. Peretyazhko, T.S., Zhang, Q., Colvin, V.L.: Size-controlled dissolution of silver nanoparticles at neutral and acidic pH conditions: kinetics and size changes. *Environ. Sci. Technol.* **48**(20), 11954–11961 (2014)
25. Larson, T.A., Joshi, P.P., Sokolov, K.: Preventing protein adsorption and macrophage uptake of gold nanoparticles via a hydrophobic shield. *ACS Nano* **6**(10), 9182–9190 (2012)
26. Urban, D.A., Rodriguez-Lorenzo, L., Balog, S., Kinnear, C., Rothen-Rutishauser, B., Petri-Fink, A.: Plasmonic nanoparticles and their characterization in physiological fluids. *Colloid Surf. B* **137**, 39–49 (2016)
27. Kreyling, W.G., Abdelmonem, A.M., Ali, Z., Alves, F., Geiser, M., Haberl, N., Hartmann, R., Hirn, S., de Aberasturi, D.J., Kantner, K., Khadem-Saba, G., Montenegro, J.-M., Rejman, J., Rojo, T., de Larramendi, I.R., Ufartes, R., Wenk, A., Parak, W.J.: In vivo integrity of polymer-coated gold nanoparticles. *Nat. Nanotechnol.* **10**, 619 (2015)
28. Lynch, I., Langevin, D., Dawson, K.A.: Lessons for bionanointeractions from colloidal science. In: Starov, V.M. (ed.) *Nanoscience: Colloidal and Interfacial Aspects*, p. 369. Taylor & Francis, London (2010)
29. Cedervall, T., Lynch, I., Lindman, S., Berggård, T., Thulin, E., Nilsson, H., Dawson, K.A., Linse, S.: Understanding the nanoparticle–protein corona using methods to quantify exchange rates and affinities of proteins for nanoparticles. *Proc. Natl. Acad. Sci. U. S. A.* **104**(7), 2050 (2007)

30. Walkey, C.D., Olsen, J.B., Song, F., Liu, R., Guo, H., Olsen, D.W.H., Cohen, Y., Emili, A., Chan, W.C.W.: Protein corona fingerprinting predicts the cellular interaction of gold and silver nanoparticles. *ACS Nano* **8**(3), 2439–2455 (2014)
31. Liu, R., Jiang, W., Walkey, C.D., Chan, W.C.W., Cohen, Y.: Prediction of nanoparticles-cell association based on corona proteins and physicochemical properties. *Nanoscale* **7**(21), 9664–9675 (2015)
32. Ke, P.C., Lin, S., Parak, W.J., Davis, T.P., Caruso, F.: A decade of the protein corona. *ACS Nano* **11**(12), 11773–11776 (2017)
33. Treuel, L., Docter, D., Maskos, M., Stauber, R.H.: Protein corona—from molecular adsorption to physiological complexity. *Beilstein J. Nanotech.* **6**, 857–873 (2015)
34. Medintz, I.L., Konnert, J.H., Clapp, A.R., Stanish, I., Twigg, M.E., Mattoussi, H., Mauro, J.M., Deschamps, J.R.: A fluorescence resonance energy transfer-derived structure of a quantum dot-protein bioconjugate nanoassembly. *Proc. Natl. Acad. Sci. U. S. A.* **101**(26), 9612–9617 (2004)
35. Schein, C.H.: Solubility as a function of protein structure and solvent components. *Bio/Technology* **8**, 308 (1990)
36. Monopoli, M.P., Åberg, C., Salvati, A., Dawson, K.A.: Biomolecular coronas provide the biological identity of nanosized materials. *Nat. Nanotechnol.* **7**, 779 (2012)
37. Docter, D., Westmeier, D., Markiewicz, M., Stolte, S., Knauer, S.K., Stauber, R.H.: The nanoparticle biomolecule corona: lessons learned—challenge accepted? *Chem. Soc. Rev.* **44**(17), 6094–6121 (2015)
38. Monopoli, M.P., Wan, S., Bombelli, F.B., Mahon, E., Dawson, K.A.: Comparisons of nanoparticle protein corona complexes isolated with different methods. *Nano Life* **03**(04), 1343004 (2013)
39. Weber, C., Simon, J., Mailänder, V., Morsbach, S., Landfester, K.: Preservation of the soft protein corona in distinct flow allows identification of weakly bound proteins. *Acta Biomater.* **76**, 217–224 (2018)
40. Lück, M., Paulke, B.-R., Schröder, W., Blunk, T., Müller, R.H.: Analysis of plasma protein adsorption on polymeric nanoparticles with different surface characteristics. *J. Biomed. Mater. Res.* **39**(3), 478–485 (1998)
41. Gessner, A., Lieske, A., Paulke, B.-R., Müller, R.H.: Functional groups on polystyrene model nanoparticles: influence on protein adsorption. *J. Biomed. Mater. Res. Part A* **65A**(3), 319–326 (2003)
42. Tenzer, S., Docter, D., Kuharev, J., Musyanovych, A., Fetz, V., Hecht, R., Schlenk, F., Fischer, D., Kiouptsi, K., Reinhardt, C., Landfester, K., Schild, H., Maskos, M., Knauer, S.K., Stauber, R.H.: Rapid formation of plasma protein corona critically affects nanoparticle pathophysiology. *Nat. Nanotechnol.* **8**, 772 (2013)
43. Zhdanov, V.P., Cho, N.-J.: Kinetics of the formation of a protein corona around nanoparticles. *Math. Biosci.* **282**, 82–90 (2016)
44. Vroman, L., Adams, A.L.: Identification of rapid changes at plasma–solid interfaces. *J. Biomed. Mater. Res.* **3**(1), 43–67 (1969)
45. Ritz, S., Schöttler, S., Kotman, N., Baier, G., Musyanovych, A., Kuharev, J., Landfester, K., Schild, H., Jahn, O., Tenzer, S., Mailänder, V.: Protein corona of nanoparticles: distinct proteins regulate the cellular uptake. *Biomacromolecules* **16**(4), 1311–1321 (2015)
46. Owens, D.E., Peppas, N.A.: Opsonization, biodistribution, and pharmacokinetics of polymeric nanoparticles. *Int. J. Pharmaceut.* **307**(1), 93–102 (2006)
47. Schöttler, S., Becker, G., Winzen, S., Steinbach, T., Mohr, K., Landfester, K., Mailänder, V., Wurm, F.R.: Protein adsorption is required for stealth effect of poly(ethylene glycol)- and poly(phosphoester)-coated nanocarriers. *Nat. Nanotechnol.* **11**, 372 (2016)
48. Perry, J.L., Reuter, K.G., Kai, M.P., Herlihy, K.P., Jones, S.W., Luft, J.C., Napier, M., Bear, J.E., DeSimone, J.M.: PEGylated PRINT nanoparticles: the impact of PEG density on protein binding, macrophage association, biodistribution, and pharmacokinetics. *Nano Lett.* **12**(10), 5304–5310 (2012)

49. Sacchetti, C., Motamedchaboki, K., Magrini, A., Palmieri, G., Mattei, M., Bernardini, S., Rosato, N., Bottini, N., Bottini, M.: Surface polyethylene glycol conformation influences the protein corona of polyethylene glycol-modified single-walled carbon nanotubes: potential implications on biological performance. *ACS Nano* **7**(3), 1974–1989 (2013)
50. Gref, R., Lück, M., Quellec, P., Marchand, M., Dellacherie, E., Harnisch, S., Blunk, T., Müller, R.H.: ‘Stealth’ corona-core nanoparticles surface modified by polyethylene glycol (PEG): influences of the corona (PEG chain length and surface density) and of the core composition on phagocytic uptake and plasma protein adsorption. *Colloids Surf. B Biointerfaces* **18**(3–4), 301–313 (2000)
51. Müller, J., Simon, J., Rohne, P., Koch-Brandt, C., Mailänder, V., Morsbach, S., Landfester, K.: Denaturation via surfactants changes composition of protein corona. *Biomacromolecules* **19**(7), 2657–2664 (2018)
52. Müller, J., Bauer, K.N., Prozeller, D., Simon, J., Mailänder, V., Wurm, F.R., Winzen, S., Landfester, K.: Coating nanoparticles with tunable surfactants facilitates control over the protein corona. *Biomaterials* **115**, 1–8 (2017)
53. Schäffler, M., Semmler-Behnke, M., Sarioglu, H., Takenaka, S., Wenk, A., Schleh, C., Hauck, S.M., Johnston, B.D., Kreyling, W.G.: Serum protein identification and quantification of the corona of 5, 15 and 80 nm gold nanoparticles. *Nanotechnology* **24**(26), 265103 (2013)
54. Miclăuş, T., Bochenkov, V.E., Ogaki, R., Howard, K.A., Sutherland, D.S.: Spatial mapping and quantification of soft and hard protein coronas at silver nanocubes. *Nano Lett.* **14**(4), 2086–2093 (2014)
55. Zhou, J.D., Gysell, M., Tara, S., Anthony, M., Darren, M., Rodney, F.M.: Differential plasma protein binding to metal oxide nanoparticles. *Nanotechnology* **20**(45), 455101 (2009)
56. Feiner-Gracia, N., Beck, M., Pujals, S., Tosi, S., Mandal, T., Buske, C., Linden, M., Albertazzi, L.: Super-resolution microscopy unveils dynamic heterogeneities in nanoparticle protein corona. *Small* **13**(41), 1701631–n/a (2017)
57. Welsher, K., Liu, Z., Sherlock, S.P., Robinson, J.T., Chen, Z., Daranciang, D., Dai, H.: A route to brightly fluorescent carbon nanotubes for near-infrared imaging in mice. *Nat. Nanotechnol.* **4**, 773 (2009)
58. Wan, S., Kelly, P.M., Mahon, E., Stöckmann, H., Rudd, P.M., Caruso, F., Dawson, K.A., Yan, Y., Monopoli, M.P.: The “Sweet” side of the protein corona: effects of glycosylation on nanoparticle-cell interactions. *ACS Nano* **9**(2), 2157–2166 (2015)
59. Lynch, I., Dawson, K.A.: Protein-nanoparticle interactions. *Nano Today* **3**(1), 40–47 (2008)
60. Nguyen, V.H., Lee, B.-J.: Protein corona: a new approach for nanomedicine design. *Int. J. Nanomed.* **12**, 3137–3151 (2017)
61. Patel, H.M.: Serum opsonins and liposomes: their interaction and opsonophagocytosis. *Crit. Rev. Ther. Drug Carrier Syst.* **9**(1), 39–90 (1992)
62. Chonn, A., Semple, S.C., Cullis, P.R.: Association of blood proteins with large unilamellar liposomes in vivo. Relation to circulation lifetimes. *J. Biol. Chem.* **267**(26), 18759–18765 (1992)
63. Tyrrell, D.A., Richardson, V.J., Ryman, B.E.: The effect of serum protein fractions on liposome-cell interactions in cultured cells and the perfused rat liver. *Biochim. Biophys. Acta (BBA) Gen. Subj.* **497**(2), 469–480 (1977)
64. Göppert, T.M., Müller, R.H.: Polysorbate-stabilized solid lipid nanoparticles as colloidal carriers for intravenous targeting of drugs to the brain: comparison of plasma protein adsorption patterns. *J. Drug Target.* **13**(3), 179–187 (2005)
65. Mirshafiee, V., Kim, R., Park, S., Mahmoudi, M., Kraft, M.L.: Impact of protein pre-coating on the protein corona composition and nanoparticle cellular uptake. *Biomaterials* **75**, 295–304 (2016)
66. Moghimi, S.M., Hunter, A.C., Murray, J.C.: Long-circulating and target-specific nanoparticles: theory to practice. *Pharmacol. Rev.* **53**(2), 283–318 (2001)
67. Corbo, C., Molinaro, R., Parodi, A., Toledano Furman, N.E., Salvatore, F., Tasciotti, E.: The impact of nanoparticle protein corona on cytotoxicity, immunotoxicity and target drug delivery. *Nanomedicine* **11**(1), 81–100 (2016)

68. Salvati, A., Pitek, A.S., Monopoli, M.P., Prapainop, K., Bombelli, F.B., Hristov, D.R., Kelly, P.M., Åberg, C., Mahon, E., Dawson, K.A.: Transferrin-functionalized nanoparticles lose their targeting capabilities when a biomolecule corona adsorbs on the surface. *Nat. Nanotechnol.* **8**, 137 (2013)
69. Landgraf, L., Christner, C., Storck, W., Schick, I., Krumbein, I., Dähring, H., Haedicke, K., Heinz-Herrmann, K., Teichgräber, U., Reichenbach, J.R., Tremel, W., Tenzer, S., Hilger, I.: A plasma protein corona enhances the biocompatibility of Au@Fe₃O₄ Janus particles. *Biomaterials* **68**, 77–88 (2015)
70. Ge, C., Du, J., Zhao, L., Wang, L., Liu, Y., Li, D., Yang, Y., Zhou, R., Zhao, Y., Chai, Z., Chen, C.: Binding of blood proteins to carbon nanotubes reduces cytotoxicity. *Proc. Natl. Acad. Sci. U. S. A.* **108**(41), 16968–16973 (2011)
71. Wang, F., Yu, L., Monopoli, M.P., Sandin, P., Mahon, E., Salvati, A., Dawson, K.A.: The biomolecular corona is retained during nanoparticle uptake and protects the cells from the damage induced by cationic nanoparticles until degraded in the lysosomes. *Nanomedicine Nanotechnol. Biol. Med.* **9**(8), 1159–1168 (2013)
72. Lee, I.S., Lee, N., Park, J., Kim, B.H., Yi, Y.-W., Kim, T., Kim, T.K., Lee, I.H., Paik, S.R., Hyeon, T.: Ni/NiO core/shell nanoparticles for selective binding and magnetic separation of histidine-tagged proteins. *JACS* **128**(33), 10658–10659 (2006)
73. Capriotti, A.L., Caracciolo, G., Cavaliere, C., Colapicchioni, V., Piovesana, S., Pozzi, D., Laganà, A.: Analytical methods for characterizing the nanoparticle-protein corona. *Chromatographia* **77**(11), 755–769 (2014)
74. Li, L., Mu, Q., Zhang, B., Yan, B.: Analytical strategies for detecting nanoparticle-protein interactions. *The Analyst* **135**(7), 1519–1530 (2010)
75. Mahmoudi, M., Lynch, I., Ejtehadi, M.R., Monopoli, M.P., Bombelli, F.B., Laurent, S.: Protein–nanoparticle interactions: opportunities and challenges. *Chem. Rev.* **111**(9), 5610–5637 (2011)
76. Aggarwal, P., Hall, J.B., McLeland, C.B., Dobrovolskaia, M.A., McNeil, S.E.: Nanoparticle interaction with plasma proteins as it relates to particle biodistribution, biocompatibility and therapeutic efficacy. *Adv. Drug Deliv. Rev.* **61**(6), 428–437 (2009)
77. Levy, R., Thanh, N.T.K., Doty, R.C., Hussain, I., Nichols, R.J., Schiffrin, D.J., Brust, M., Fernig, D.G.: Rational and combinatorial design of peptide capping Ligands for gold nanoparticles. *JACS* **126**(32), 10076–10084 (2004)
78. Aubin-Tam, M.-E., Hamad-Schifferli, K.: Gold nanoparticle–cytochrome c complexes: the effect of nanoparticle ligand charge on protein structure. *Langmuir* **21**(26), 12080–12084 (2005)
79. Ashby, J., Schachermeyer, S., Pan, S., Zhong, W.: Dissociation-based screening of nanoparticle-protein interaction via flow field-flow fractionation. *Anal. Chem.* **85**(15), 7494–7501 (2013)
80. Aleksenko, S.S., Shmykov, A.Y., Oszwaldowski, S., Timerbaev, A.R.: Interactions of tumour-targeting nanoparticles with proteins: potential of using capillary electrophoresis as a direct probe. *Metallomics* **4**(11), 1141–1148 (2012)
81. Kim, H.R., Andrieux, K., Delomenie, C., Chacun, H., Appel, M., Desmaele, D., Taran, F., Geogin, D., Couvreur, P., Taverna, M.: Analysis of plasma protein adsorption onto PEGylated nanoparticles by complementary methods: 2-DE, CE and protein Lab-on-chip(R) system. *Electrophoresis* **28**(13), 2252–2261 (2007)
82. Brambilla, D., Verpillot, R., Taverna, M., De Kimpe, L., Le Droumaguet, B., Nicolas, J., Canovi, M., Gobbi, M., Mantegazza, F., Salmona, M., Nicolas, V., Scheper, W., Couvreur, P., Andrieux, K.: New method based on capillary electrophoresis with laser-induced fluorescence detection (CE-LIF) to monitor interaction between nanoparticles and the amyloid-beta peptide. *Anal. Chem.* **82**(24), 10083–10089 (2010)
83. Brambilla, D., Verpillot, R., Le Droumaguet, B., Nicolas, J., Taverna, M., Kona, J., Lettiero, B., Hashemi, S.H., De Kimpe, L., Canovi, M., Gobbi, M., Nicolas, V., Scheper, W., Moghimi, S.M., Tvaroska, I., Couvreur, P., Andrieux, K.: PEGylated nanoparticles bind to and alter amyloid-beta peptide conformation: toward engineering of functional nanomedicines for Alzheimer’s disease. *ACS Nano* **6**(7), 5897–5908 (2012)

84. Chang, C.W., Tseng, W.L.: Gold nanoparticle extraction followed by capillary electrophoresis to determine the total, free, and protein-bound amino thiols in plasma. *Anal. Chem.* **82**(7), 2696–2702 (2010)
85. Chen, F., Wang, G., Griffin, J.I., Brenneman, B., Banda, N.K., Holers, V.M., Backos, D.S., Wu, L., Moghimi, S.M., Simberg, D.: Complement proteins bind to nanoparticle protein corona and undergo dynamic exchange in vivo. *Nat. Nanotechnol.* **12**, 387 (2016)
86. García-Álvarez, R., Hadjidemetriou, M., Sánchez-Iglesias, A., Liz-Marzán, L.M., Kostarelos, K.: In vivo formation of protein corona on gold nanoparticles. The effect of their size and shape. *Nanoscale* **10**(3), 1256–1264 (2018)
87. Caracciolo, G., Pozzi, D., De Sanctis, S.C., Capriotti, A.L., Caruso, G., Samperi, R., Lagana, A.: Effect of membrane charge density on the protein corona of cationic liposomes: interplay between cationic charge and surface area. *Appl. Phys. Lett.* **99**(3) (2011)
88. Dutta, D., Sundaram, S.K., Teegarden, J.G., Riley, B.J., Fifield, L.S., Jacobs, J.M., Addleman, S.R., Kaysen, G.A., Moudgil, B.M., Weber, T.J.: Adsorbed proteins influence the biological activity and molecular targeting of nanomaterials. *Toxicol. Sci.* **100**(1), 303–315 (2007)
89. Salvador-Morales, C., Flahaut, E., Sim, E., Sloan, J., Green, M.L., Sim, R.B.: Complement activation and protein adsorption by carbon nanotubes. *Mol. Immunol.* **43**(3), 193–201 (2006)
90. Lundqvist, M., Stigler, J., Elia, G., Lynch, I., Cedervall, T., Dawson, K.A.: Nanoparticle size and surface properties determine the protein corona with possible implications for biological impacts. *Proc. Natl. Acad. Sci. U. S. A.* **105**(38), 14265–14270 (2008)
91. Stolnik, S., Daudali, B., Arien, A., Whetstone, J., Heald, C.R., Garnett, M.C., Davis, S.S., Illum, L.: The effect of surface coverage and conformation of poly(ethylene oxide) (PEO) chains of poloxamer 407 on the biological fate of model colloidal drug carriers. *Biochim. Biophys. Acta (BBA) Biomembr.* **1514**(2), 261–279 (2001)
92. Arora, P.S., Yamagiwa, H., Srivastava, A., Bolander, M.E., Sarkar, G.: Comparative evaluation of two two-dimensional gel electrophoresis image analysis software applications using synovial fluids from patients with joint disease. *J. Orthop. Sci.* **10**(2), 160–166 (2005)
93. Lai, Z.W., Yan, Y., Caruso, F., Nice, E.C.: Emerging techniques in proteomics for probing nano-bio interactions. *ACS Nano* **6**(12), 10438–10448 (2012)
94. Kim, H.R., Andrieux, K., Gil, S., Taverna, M., Chacun, H., Desmaële, D., Taran, F., Georgin, D., Couvreur, P.: Translocation of poly(ethylene glycol-co-hexadecyl)cyanoacrylate nanoparticles into rat brain endothelial cells: role of apolipoproteins in receptor-mediated endocytosis. *Biomacromolecules* **8**(3), 793–799 (2007)
95. Chang, S.Y., Zheng, N.-Y., Chen, C.-S., Chen, C.-D., Chen, Y.-Y., Wang, C.R.C.: Analysis of peptides and proteins affinity-bound to iron oxide nanoparticles by MALDI MS. *J. Am. Soc. Mass Spectrom.* **18**(5), 910–918 (2007)
96. Chittur, K.K.: FTIR/ATR for protein adsorption to biomaterial surfaces. *Biomaterials* **19**(4), 357–369 (1998)
97. Goormaghtigh, E., Gasper, R., Bénard, A., Goldsztein, A., Raussens, V.: Protein secondary structure content in solution, films and tissues: redundancy and complementarity of the information content in circular dichroism, transmission and ATR FTIR spectra. *Biochim. Biophys. Acta (BBA) Proteins Proteomics* **1794**(9), 1332–1343 (2009)
98. Shao, M., Lu, L., Wang, H., Luo, S., Ma, D.D.D.: Microfabrication of a new sensor based on silver and silicon nanomaterials, and its application to the enrichment and detection of bovine serum albumin via surface-enhanced Raman scattering. *Microchim. Acta* **164**(1), 157–160 (2009)
99. Royer, C.A.: Probing protein folding and conformational transitions with fluorescence. *Chem. Rev.* **106**(5), 1769–1784 (2006)
100. Mátyus, L., Szöllösi, J., Jenei, A.: Steady-state fluorescence quenching applications for studying protein structure and dynamics. *J. Photochem. Photobiol. B* **83**(3), 223–236 (2006)
101. Vilanova, O., Mittag, J.J., Kelly, P.M., Milani, S., Dawson, K.A., Rädler, J.O., Franzese, G.: Understanding the kinetics of protein-nanoparticle corona formation. *ACS Nano* **10**(12), 10842–10850 (2016)

102. Kelly, S.M., Jess, T.J., Price, N.C.: How to study proteins by circular dichroism. *Biochim. Biophys. Acta (BBA) Proteins Proteomics* **1751**(2), 119–139 (2005)
103. Shang, L., Wang, Y., Jiang, J., Dong, S.: pH-dependent protein conformational changes in albumin: gold nanoparticle bioconjugates: a spectroscopic study. *Langmuir* **23**(5), 2714–2721 (2007)
104. Deng, Z.J., Liang, M., Monteiro, M., Toth, I., Minchin, R.F.: Nanoparticle-induced unfolding of fibrinogen promotes Mac-1 receptor activation and inflammation. *Nat. Nanotechnol.* **6**, 39 (2010)
105. Cecccon, A., Lelli, M., D’Onofrio, M., Molinari, H., Assfalg, M.: Dynamics of a globular protein adsorbed to liposomal nanoparticles. *JACS* **136**(38), 13158–13161 (2014)
106. Stayton, P.S., Drobny, G.P., Shaw, W.J., Long, J.R., Gilbert, M.: Molecular recognition at the protein-hydroxyapatite interface. *Crit. Rev. Oral Biol. Med.* **14**(5), 370–376 (2003)
107. Carril, M., Padro, D., del Pino, P., Carrillo-Carrion, C., Gallego, M., Parak, W.J.: In situ detection of the protein corona in complex environments. *Nat. Commun.* **8**(1), 1542 (2017)
108. Baier, G., Costa, C., Zeller, A., Baumann, D., Sayer, C., Araujo, P.H.H., Mäiländer, V., Musyanovych, A., Landfester, K.: BSA adsorption on differently charged polystyrene nanoparticles using isothermal titration calorimetry and the influence on cellular uptake. *Macromol. Biosci.* **11**(5), 628–638 (2011)
109. Lindman, S., Lynch, I., Thulin, E., Nilsson, H., Dawson, K.A., Linse, S.: Systematic investigation of the thermodynamics of HSA adsorption to N-iso-Propylacrylamide/N-tert-Butylacrylamide copolymer nanoparticles. Effects of particle size and hydrophobicity. *Nano Lett.* **7**(4), 914–920 (2007)
110. Laera, S., Cecccone, G., Rossi, F., Gilliland, D., Hussain, R., Siligardi, G., Calzolari, L.: Measuring protein structure and stability of protein-nanoparticle systems with synchrotron radiation circular dichroism. *Nano Lett.* **11**(10), 4480–4484 (2011)
111. Bhogale, A., Patel, N., Mariam, J., Dongre, P.M., Miotello, A., Kothari, D.C.: Comprehensive studies on the interaction of copper nanoparticles with bovine serum albumin using various spectroscopies. *Colloids Surf. B* **113**, 276–284 (2014)
112. Astegno, A., Maresi, E., Marino, V., Dominici, P., Pedroni, M., Piccinelli, F., Dell’Orco, D.: Structural plasticity of calmodulin on the surface of CaF₂ nanoparticles preserves its biological function. *Nanoscale* **6**(24), 15037–15047 (2014)
113. Huang, R., Carney, R.P., Ikuma, K., Stellacci, F., Lau, B.L.T.: Effects of surface compositional and structural heterogeneity on nanoparticle-protein interactions: different protein configurations. *ACS Nano* **8**(6), 5402–5412 (2014)
114. Michen, B., Geers, C., Vanhecke, D., Endes, C., Rothen-Rutishauser, B., Balog, S., Petri-Fink, A.: Avoiding drying-artifacts in transmission electron microscopy: characterizing the size and colloidal state of nanoparticles. *Sci. Rep.* **5**, 9793 (2015)
115. Balog, S., Rodriguez-Lorenzo, L., Monnier, C.A., Obiols-Rabasa, M., Rothen-Rutishauser, B., Schurtenberger, P., Petri-Fink, A.: Characterizing nanoparticles in complex biological media and physiological fluids with depolarized dynamic light scattering. *Nanoscale* **7**(14), 5991–5997 (2015)
116. Sharifi, S., Behzadi, S., Laurent, S., Laird Forrest, M., Stroeve, P., Mahmoudi, M.: Toxicity of nanomaterials. *Chem. Soc. Rev.* **41**(6), 2323–2343 (2012)
117. Lin, P.-C., Lin, S., Wang, P.C., Sridhar, R.: Techniques for physicochemical characterization of nanomaterials. *Biotechnol. Adv.* **32**(4), 711–726 (2014)
118. Treuel, L., Eslahian, K.A., Docter, D., Lang, T., Zellner, R., Nienhaus, K., Nienhaus, G.U., Stauber, R.H., Maskos, M.: Physicochemical characterization of nanoparticles and their behavior in the biological environment. *Phys. Chem. Chem. Phys.* **16**(29), 15053–15067 (2014)
119. Cho, E.C., Liu, Y., Xia, Y.: A simple spectroscopic method for differentiating cellular uptakes of gold nanospheres and nanorods from their mixtures. *Angew. Chem. Int. Ed.* **49**(11), 1976–1980 (2010)
120. Rischitor, G., Parracino, M., La Spina, R., Urbán, P., Ojea-Jiménez, I., Bellido, E., Valsesia, A., Gioria, S., Capomaccio, R., Kinsner-Ovaskainen, A., Gilliland, D., Rossi, F., Colpo, P.:

- Quantification of the cellular dose and characterization of nanoparticle transport during in vitro testing. *Part. Fibre Toxicol.* **13**(1), 47 (2016)
121. Cho, E.C., Zhang, Q., Xia, Y.: The effect of sedimentation and diffusion on cellular uptake of gold nanoparticles. *Nat. Nanotechnol.* **6**, 385 (2011)
 122. Mukherjee, D., Leo, B.F., Royce, S.G., Porter, A.E., Ryan, M.P., Schwander, S., Chung, K.F., Tetley, T.D., Zhang, J., Georgopoulos, P.G.: Modeling physicochemical interactions affecting in vitro cellular dosimetry of engineered nanomaterials: application to nanosilver. *J. Nanopart. Res.* **16**(10), 2616 (2014)
 123. Hinderliter, P.M., Minard, K.R., Orr, G., Chrisler, W.B., Thrall, B.D., Pounds, J.G., Tee-guarden, J.G.: ISDD: a computational model of particle sedimentation, diffusion and target cell dosimetry for in vitro toxicity studies. *Part. Fibre Toxicol.* **7**(1), 36 (2010)
 124. DeLoid, G., Cohen, J.M., Darrach, T., Derk, R., Rojanasakul, L., Pyrgiotakis, G., Wohlleben, W., Demokritou, P.: Estimating the effective density of engineered nanomaterials for in vitro dosimetry. *Nat. Commun.* **5**, 3514 (2014)
 125. DeLoid, G.M., Cohen, J.M., Pyrgiotakis, G., Pirella, S.V., Pal, A., Liu, J., Srebric, J., Demokritou, P.: Advanced computational modeling for in vitro nanomaterial dosimetry. *Part. Fibre Toxicol.* **12**, 32 (2015)
 126. Rodriguez-Lorenzo, L., Rothen-Rutishauser, B., Petri-Fink, A., Balog, S.: Nanoparticle polydispersity can strongly affect in vitro dose. *Part. Part. Syst. Charact.* **32**(3), 321–333 (2015)
 127. Thomas, D.G., Smith, J.N., Thrall, B.D., Baer, D.R., Jolley, H., Munusamy, P., Kodali, V., Demokritou, P., Cohen, J., Teeguarden, J.G.: ISD3: a particokinetic model for predicting the combined effects of particle sedimentation, diffusion and dissolution on cellular dosimetry for in vitro systems. *Part. Fibre Toxicol.* **15**(1), 6 (2018)
 128. Zhang, S., Li, J., Lykotraftits, G., Bao, G., Suresh, S.: Size-dependent endocytosis of nanoparticles. *Adv. Mater.* **21**(4), 419–424 (2009)
 129. Abhishek, C., Giuseppe, B., Ramin, G.: The effect of interactions on the cellular uptake of nanoparticles. *Phys. Biol.* **8**(4), 046002 (2011)
 130. Kinnear, C., Moore, T.L., Rodriguez-Lorenzo, L., Rothen-Rutishauser, B., Petri-Fink, A.: Form follows function: nanoparticle shape and its implications for nanomedicine. *Chem. Rev.* **117**(17), 11476–11521 (2017)
 131. Sadik, O.A.: Anthropogenic nanoparticles in the environment. *Environ. Sci. Process. Impacts* **15**(1), 19–20 (2013)
 132. Buzea, C., Pacheco, I.I., Robbie, K.: Nanomaterials and nanoparticles: sources and toxicity. *Biointerphases* **2**(4), Mr17–Mr71 (2007)
 133. Kuhlbusch, T., Asbach, C., Fissan, H., Gohler, D., Stintz, M.: Nanoparticle exposure at nanotechnology workplaces: a review. *Part. Fibre Toxicol.* **8**(1), 22 (2011)
 134. Drasler, B., Sayre, P., Steinhauser, K.G., Petri-Fink, A., Rothen-Rutishauser, B.: In vitro approaches to assess the hazard of nanomaterials. *Nanoimpact* **8**, 99–116 (2017)
 135. Mühlfeld, C., Rothen-Rutishauser, B., Blank, F., Vanhecke, D., Ochs, M., Gehr, P.: Interactions of nanoparticles with pulmonary structures and cellular responses. *AJP-Lung* **294**(5), L817–L829 (2008)
 136. Conner, S.D., Schmid, S.L.: Regulated portals of entry into the cell. *Nature* **422**, 37 (2003)
 137. Aderem, A., Underhill, D.M.: Mechanisms of phagocytosis in macrophages. *Annu. Rev. Immunol.* **17**(1), 593–623 (1999)
 138. Spector, A.A., Yorek, M.A.: Membrane lipid composition and cellular function. *J. Lipid Res.* **26**(9), 1015–1035 (1985)
 139. Kuhn, D.A., Vanhecke, D., Michen, B., Blank, F., Gehr, P., Petri-Fink, A., Rothen-Rutishauser, B.: Different endocytotic uptake mechanisms for nanoparticles in epithelial cells and macrophages. *Beilstein J. Nanotech.* **5**, 1625–1636 (2014)
 140. Mahmoudi, M., Saeedi-Eslami, S.N., Shokrgozar, M.A., Azadmanesh, K., Hassanlou, M., Kalhor, H.R., Burtea, C., Rothen-Rutishauser, B., Laurent, S., Sheibani, S., Vali, H.: Cell “vision”: complementary factor of protein corona in nanotoxicology. *Nanoscale* **4**(17), 5461–5468 (2012)

141. Feliu, N., Hühn, J., Zyuzin, M.V., Ashraf, S., Valdeperez, D., Masood, A., Said, A.H., Escudero, A., Pelaz, B., Gonzalez, E., Duarte, M.A.C., Roy, S., Chakraborty, I., Lim, M.L., Sjöqvist, S., Jungebluth, P., Parak, W.J.: Quantitative uptake of colloidal particles by cell cultures. *Sci. Total Environ.* **568**, 819–828 (2016)
142. Donaldson, K., Stone, V., Borm, P.J.A., Jimenez, L.A., Gilmour, P.S., Schins, R.P.F., Knaapen, A.M., Rahman, I., Faux, S.P., Brown, D.M., MacNee, W.: Oxidative stress and calcium signaling in the adverse effects of environmental particles (PM10). *Free Radic. Biol. Med.* **34**(11), 1369–1382 (2003)
143. Poland, C.A., Duffin, R., Kinloch, I., Maynard, A., Wallace, W.A.H., Seaton, A., Stone, V., Brown, S., MacNee, W., Donaldson, K.: Carbon nanotubes introduced into the abdominal cavity of mice show asbestos-like pathogenicity in a pilot study. *Nat. Nanotechnol.* **3**, 423 (2008)
144. Schins, R.P.F., Knaapen, A.M.: Genotoxicity of poorly soluble particles. *Inhal. Toxicol.* **19**(sup1), 189–198 (2007)
145. Krug, H.F., Wick, P.: Nanotoxicology: an interdisciplinary challenge. *Angew. Chem. Int. Ed.* **50**(6), 1260–1278 (2011)
146. Paur, H.-R., Cassee, F.R., Teeguarden, J., Fissan, H., Diabate, S., Aufderheide, M., Kreyling, W.G., Hänninen, O., Kasper, G., Riediker, M., Rothen-Rutishauser, B., Schmid, O.: In-vitro cell exposure studies for the assessment of nanoparticle toxicity in the lung—a dialog between aerosol science and biology. *J. Aerosol Sci.* **42**(10), 668–692 (2011)
147. Bourquin, J., Milosevic, A., Hauser, D., Lehner, R., Blank, F., Petri-Fink, A., Rothen-Rutishauser, B.: Biodistribution, clearance, and long-term fate of clinically relevant nanomaterials. *Adv. Mater.*, 1704307 (2018)
148. Geers, C., Rodriguez-Lorenzo, L., Andreas Urban, D., Kinnear, C., Petri-Fink, A., Balog, S.: A new angle on dynamic depolarized light scattering: number-averaged size distribution of nanoparticles in focus. *Nanoscale* **8**(34), 15813–15821 (2016)
149. Mehan, S., Chinchalikar, A.J., Kumar, S., Aswal, V.K., Schweins, R.: Small-angle neutron scattering study of structure and interaction of nanoparticle, protein, and surfactant complexes. *Langmuir* **29**(36), 11290–11299 (2013)
150. Spinozzi, F., Ceccone, G., Moretti, P., Campanella, G., Ferrero, C., Combet, S., Ojea-Jimenez, I., Ghigna, P.: Structural and thermodynamic properties of nanoparticle-protein complexes: a combined SAXS and SANS study. *Langmuir* **33**(9), 2248–2256 (2017)
151. Diroll, B.T., Weigandt, K.M., Jishkariani, D., Cargnello, M., Murphy, R.J., Hough, L.A., Murray, C.B., Donnio, B.: Quantifying “Softness” of organic coatings on gold nanoparticles using correlated small-angle X-ray and neutron scattering. *Nano Lett.* **15**(12), 8008–8012 (2015)
152. Bhattacharjee, S.: DLS and zeta potential—what they are and what they are not? *J. Contr. Release* **235**, 337–351 (2016)
153. Huang, Y., Wang, X.B., Becker, F.F., Gascoyne, P.R.: Introducing dielectrophoresis as a new force field for field-flow fractionation. *Biophys. J.* **73**(2), 1118–1129 (1997)
154. Uma, B., Swaminathan, T.N., Radhakrishnan, R., Eckmann, D.M., Ayyaswamy, P.S.: Nanoparticle Brownian motion and hydrodynamic interactions in the presence of flow fields. *Phys. Fluids* **23**(7), 073602 (2011)
155. Das, S., Kundu, A., Hossain, S.M., Saha, H., Datta, S.K.: Effect of size on the scattering properties of silica nanoparticles. In: 2014 IEEE 2nd International Conference on Emerging Electronics (ICEE), 3–6 December 2014, pp. 1–4 (2014)
156. Horiba Instruments, I.: Zeta Potential of Bovine Serum Albumin (BSA) Protein. Irvine, CA, U.S.A (2009)
157. Vanhecke, D., Kuhn, D.A., Jimenez de Aberasturi, D., Balog, S., Milosevic, A., Urban, D., Peckys, D., de Jonge, N., Parak, W.J., Petri-Fink, A., Rothen-Rutishauser, B.: Involvement of two uptake mechanisms of gold and iron oxide nanoparticles in a co-exposure scenario using mouse macrophages. *Beilstein J. Nanotechnol.* **8**, 2396–2409 (2017)
158. Nuhn, L., Gietzen, S., Mohr, K., Fischer, K., Toh, K., Miyata, K., Matsumoto, Y., Kataoka, K., Schmidt, M., Zentel, R.: Aggregation behavior of cationic nanohydrogel particles in human blood serum. *Biomacromolecules* **15**(4), 1526–1533 (2014)

159. Rausch, K., Reuter, A., Fischer, K., Schmidt, M.: Evaluation of nanoparticle aggregation in human blood serum. *Biomacromolecules* **11**(11), 2836–2839 (2010)
160. Hemmelmann, M., Mohr, K., Fischer, K., Zentel, R., Schmidt, M.: Interaction of pH-MA-pLMA copolymers with human blood serum and its components. *Mol. Pharm.* **10**(10), 3769–3775 (2013)
161. Barisik, M., Atalay, S., Beskok, A., Qian, S.: Size dependent surface charge properties of silica nanoparticles. *J. Phys. Chem. C* **118**(4), 1836–1842 (2014)
162. Durantie, E., Vanhecke, D., Rodriguez-Lorenzo, L., Delhaes, F., Balog, S., Septiadi, D., Bourquin, J., Petri-Fink, A., Rothen-Rutishauser, B.: Biodistribution of single and aggregated gold nanoparticles exposed to the human lung epithelial tissue barrier at the air-liquid interface. *Part. Fibre Toxicol.* **14**(1), 49 (2017)
163. Balog, S., Rodriguez-Lorenzo, L., Monnier, C.A., Michen, B., Obiols-Rabasa, M., Casal-Dujat, L., Rothen-Rutishauser, B., Petri-Fink, A., Schurtenberger, P.: Dynamic depolarized light scattering of small round plasmonic nanoparticles: when imperfection is only perfect. *J. Phys. Chem. C* **118**(31), 17968–17974 (2014)
164. Hirsch, V., Kinnear, C., Rodriguez-Lorenzo, L., Monnier, C.A., Rothen-Rutishauser, B., Balog, S., Petri-Fink, A.: In vitro dosimetry of agglomerates. *Nanoscale* **6**(13), 7325–7331 (2014)
165. Pal, N., Verma, S.D., Singh, M.K., Sen, S.: Fluorescence correlation spectroscopy: an efficient tool for measuring size, size-distribution and polydispersity of microemulsion droplets in solution. *Anal. Chem.* **83**(20), 7736–7744 (2011)
166. Shang, L., Nienhaus, G.U.: In situ characterization of protein adsorption onto nanoparticles by fluorescence correlation spectroscopy. *Acc. Chem. Res.* **50**(2), 387–395 (2017)
167. Milosevic, A.M., Rodriguez-Lorenzo, L., Balog, S., Monnier, C.A., Petri-Fink, A., Rothen-Rutishauser, B.: Assessing the stability of fluorescently encoded nanoparticles in lysosomes by using complementary methods. *Angew. Chem. Int. Ed. Engl.* **56**(43), 13382–13386 (2017)
168. Silvestri, A., Di Silvio, D., Llarena, I., Murray, R.A., Marelli, M., Lay, L., Polito, L., Moya, S.E.: Influence of surface coating on the intracellular behaviour of gold nanoparticles: a fluorescence correlation spectroscopy study. *Nanoscale* **9**(38), 14730–14739 (2017)
169. Yang, W., Lu, J., Gilbert, E.P., Knott, R., He, L., Cheng, W.: Probing soft corona structures of DNA-capped nanoparticles by small angle neutron scattering. *J. Phys. Chem. C* **119**(32), 18773–18778 (2015)
170. Camarero-Espinosa, S., Endes, C., Mueller, S., Petri-Fink, A., Rothen-Rutishauser, B., Weder, C., Clift, M.J.D., Foster, E.J.: Elucidating the potential biological impact of cellulose nanocrystals. *Fibers* **4**(3) (2016)
171. Kinnear, C., Balog, S., Rothen-Rutishauser, B., Petri-Fink, A.: Thermally reversible self-assembly of nanoparticles via polymer crystallization. *Macromol. Rapid Commun.* **35**(23), 2012–2017 (2014)
172. Dorofeev, G.A., Streletskii, A.N., Povstugar, I.V., Protasov, A.V., Elsukov, E.P.: Determination of nanoparticle sizes by X-ray diffraction. *Colloid J.* **74**(6), 675–685 (2012)
173. Urban, D.A., Milosevic, A.M., Bossert, D., Crippa, F., Moore, T.L., Geers, C., Balog, S., Rothen-Rutishauser, B., Petri-Fink, A.: Taylor dispersion of inorganic nanoparticles and comparison to dynamic light scattering and transmission electron microscopy. *Colloid Interface Sci. Commun.* **22**, 29–33 (2018)
174. Balog, S., Urban, D.A., Milosevic, A.M., Crippa, F., Rothen-Rutishauser, B., Petri-Fink, A.: Taylor dispersion of nanoparticles. *J. Nanopart. Res.* **19**(8) (2017)
175. Zhang, D., Neumann, O., Wang, H., Yuwono, V.M., Barhoumi, A., Perham, M., Hartgerink, J.D., Wittung-Stafshede, P., Halas, N.J.: Gold nanoparticles can induce the formation of protein-based aggregates at physiological pH. *Nano Lett.* **9**(2), 666–671 (2009)
176. Bekdemir, A., Stellacci, F.: A centrifugation-based physicochemical characterization method for the interaction between proteins and nanoparticles. *Nat. Commun.* **7**, 13121 (2016)
177. Walter, J., Löhr, K., Karabudak, E., Reis, W., Mikhael, J., Peukert, W., Wohlleben, W., Cölfen, H.: Multidimensional analysis of nanoparticles with highly disperse properties using multi-wavelength analytical ultracentrifugation. *ACS Nano* **8**(9), 8871–8886 (2014)

178. Ashby, J., Pan, S., Zhong, W.: Size and surface functionalisation of iron oxide nanoparticles influence the composition and dynamic nature of their protein corona. *ACS Appl. Mater. Interfaces* **6**(17), 15412–15419 (2014)
179. Zook, J.M., Rastogi, V., MacCuspie, R.I., Keene, A.M., Fagan, J.: Measuring agglomerate size distribution and dependence of localized surface plasmon resonance absorbance on gold nanoparticle agglomerate size using analytical ultracentrifugation. *ACS Nano* **5**(10), 8070–8079 (2011)
180. Planken, K.L., Colfen, H.: Analytical ultracentrifugation of colloids. *Nanoscale* **2**(10), 1849–1869 (2010)
181. Gigault, J., Pettibone, J.M., Schmitt, C., Hackley, V.A.: Rational strategy for characterization of nanoscale particles by asymmetric-flow field flow fractionation: a tutorial. *Anal. Chim. Acta* **809**, 9–24 (2014)
182. Kozak, D., Anderson, W., Vogel, R., Trau, M.: Advances in resistive pulse sensors: devices bridging the void between molecular and microscopic detection. *Nano Today* **6**(5), 531–545 (2011)
183. Blundell, E.L.C.J., Healey, M.J., Holton, E., Sivakumaran, M., Manstana, S., Platt, M.: Characterisation of the protein corona using tunable resistive pulse sensing: determining the change and distribution of a particle's surface charge. *Anal. Bioanal. Chem.* **408**(21), 5757–5768 (2016)
184. Sikora, A., Shard, A.G., Minelli, C.: Size and ζ -potential measurement of silica nanoparticles in serum using tunable resistive pulse sensing. *Langmuir* **32**(9), 2216–2224 (2016)
185. Cipelletti, L., Biron, J.-P., Martin, M., Cottet, H.: Polydispersity analysis of taylor dispersion data: the cumulant method. *Anal. Chem.* **86**(13), 6471–6478 (2014)
186. Balog, S.: Taylor dispersion of polydisperse nanoclusters and nanoparticles: modeling, simulation, and analysis. *Anal. Chem.* (2018)
187. Dominguez, D., Alhusain, M., Alharbi, N., Bernussi, A., Grave de Peralta, L.: Fourier plane imaging microscopy for detection of plasmonic crystals with periods beyond the optical diffraction limit, vol. 10 (2015)
188. Gustafsson, M.G.L.: Surpassing the lateral resolution limit by a factor of two using structured illumination microscopy. *J. Microsc.* **198**(2), 82–87 (2000)
189. Chang, B.-J., Lin, S.H., Chou, L.-J., Chiang, S.-Y.: Subdiffraction scattered light imaging of gold nanoparticles using structured illumination. *Opt. Lett.* **36**(24), 4773–4775 (2011)
190. Vainrub, A., Pustovyy, O., Vodyanoy, V.: Resolution of 90 nm ($\lambda/5$) in an optical transmission microscope with an annular condenser. *Opt. Lett.* **31**(19), 2855–2857 (2006)
191. Guttenberg, M., Bezerra, L., Neu-Baker, N.M., del Pilar Sosa Peña, M., Elder, A., Oberdörster, G., Brenner, S.A.: Biodistribution of inhaled metal oxide nanoparticles mimicking occupational exposure: a preliminary investigation using enhanced darkfield microscopy. *J. Biophotonics* **9**(10), 987–993 (2016)
192. Peña, M.D.P.S., Gottipati, A., Tahiliani, S., Neu-Baker, N.M., Frame, M.D., Friedman, A.J., Brenner, S.A.: Hyperspectral imaging of nanoparticles in biological samples: simultaneous visualization and elemental identification. *Microsc. Res. Tech.* **79**(5), 349–358 (2016)
193. Monnier, C.A., Lattuada, M., Burnand, D., Crippa, F., Martinez-Garcia, J.C., Hirt, A.M., Rothen-Rutishauser, B., Bonmarin, M., Petri-Fink, A.: A lock-in-based method to examine the thermal signatures of magnetic nanoparticles in the liquid, solid and aggregated states. *Nanoscale* **8**(27), 13321–13332 (2016)
194. Drasler, B., Vanhecke, D., Rodriguez-Lorenzo, L., Petri-Fink, A., Rothen-Rutishauser, B.: Quantifying nanoparticle cellular uptake: which method is best? *Nanomedicine* **12**(10), 1095–1099 (2017)
195. Vanhecke, D., Rodriguez-Lorenzo, L., Clift, M.J.D., Blank, F., Petri-Fink, A., Rothen-Rutishauser, B.: Quantification of nanoparticles at the single-cell level: an overview about state-of-the-art techniques and their limitations. *Nanomedicine* **9**(12), 1885–1900 (2014)
196. Thieme, J., McNult, I., Vogt, S., Paterson, D.: X-ray spectromicroscopy—a tool for environmental sciences. *Environ. Sci. Technol.* **41**(20), 6885–6889 (2007)

197. Lawrence, J., Dynes, J., Korber, D., Swerhone, G., Leppard, G., Hitchcock, A.P.: Monitoring the fate of copper nanoparticles in river biofilms using scanning transmission X-ray microscopy (STXM), vol. 329, pp. 18–25 (2011)
198. Takechi-Haraya, Y., Goda, Y., Sakai-Kato, K.: Imaging and size measurement of nanoparticles in aqueous medium by use of atomic force microscopy. *Anal. Bioanal. Chem.* **410**(5), 1525–1531 (2018)
199. Cazaux, J.: Material contrast in SEM: fermi energy and work function effects. *Ultramicroscopy* **110**(3), 242–253 (2010)
200. Kisielowski, C., Freitag, B., Bischoff, M., van Lin, H., Lazar, S., Knippels, G., Tiemeijer, P., van der Stam, M., von Harrach, S., Stekelenburg, M., Haider, M., Uhlemann, S., Müller, H., Hartel, P., Kabius, B., Miller, D., Petrov, I., Olson, E.A., Donchev, T., Kenik, E.A., Lupini, A.R., Bentley, J., Pennycook, S.J., Anderson, I.M., Minor, A.M., Schmid, A.K., Duden, T., Radmilovic, V., Ramasse, Q.M., Watanabe, M., Erni, R., Stach, E.A., Denes, P., Dahmen, U.: Detection of single atoms and buried defects in three dimensions by aberration-corrected electron microscope with 0.5-Å information limit. *Microsc. Microanal.* **14**(5), 469–477 (2008)
201. Liu, J.: Scanning transmission electron microscopy and its application to the study of nanoparticles and nanoparticle systems. *J. Electron. Microsc.* **54**(3), 251–278 (2005)
202. Michen, B., Geers, C., Vanhecke, D., Endes, C., Rothen-Rutishauser, B., Balog, S., Petri-Fink, A.: Avoiding drying-artifacts in transmission electron microscopy: characterizing the size and colloidal state of nanoparticles. *Sci. Rep.* **5** (2015)
203. Ahmad, N., Wang, G., Nelayah, J., Ricolleau, C., Alloyeau, D.: Exploring the formation of symmetric gold nanostars by liquid-cell transmission electron microscopy. *Nano Lett.* **17**(7), 4194–4201 (2017)
204. Milosevic, A.M., Rodriguez-Lorenzo, L., Balog, S., Monnier, C.A., Petri-Fink, A., Rothen-Rutishauser, B.: Assessing the stability of fluorescently encoded nanoparticles in lysosomes by using complementary methods. *Angew. Chem. Int. Ed.* **56**(43), 13382–13386 (2017)
205. Dillon, J.C.K., Bezerra, L., del Pilar Sosa Peña, M., Neu-Baker, N.M., Brenner, S.A.: Hyper-spectral data influenced by sample matrix: the importance of building relevant reference spectral libraries to map materials of interest. *Microsc. Res. Tech.* **80**(5), 462–470 (2017)
206. Mühlfeld, C., Rothen-Rutishauser, B., Vanhecke, D., Blank, F., Gehr, P., Ochs, M.: Visualization and quantitative analysis of nanoparticles in the respiratory tract by transmission electron microscopy. *Part. Fibre Toxicol.* **4**(1), 11 (2007)
207. Gundersen, H.J.G., Jensen, E.B.: The efficiency of systematic sampling in stereology and its prediction. *J. Microsc.* **147**(3), 229–263 (1987)
208. Slack, S.M., Horbett, T.A.: The Vroman effect. In: *Proteins at Interfaces II*, American Chemical Society, vol. 602, pp. 112–128 (1995)
209. Casals, E., Pfaller, T., Duschl, A., Oostingh, G.J., Puntès, V.: Time evolution of the nanoparticle protein corona. *ACS Nano* **4**(7), 3623–3632 (2010)
210. Vroman, L.: Effect of adsorbed proteins on the wettability of hydrophilic and hydrophobic solids. *Nature* **196**, 476 (1962)
211. Li, T., Senesi, A.J., Lee, B.: Small angle X-ray scattering for nanoparticle research. *Chem. Rev.* **116**(18), 11128–11180 (2016)
212. Fong, W.K., Salentinig, S., Prestidge, C.A., Mezzenga, R., Hawley, A., Boyd, B.J.: Generation of geometrically ordered lipid-based liquid-crystalline nanoparticles using biologically relevant enzymatic processing. *Langmuir* **30**(19), 5373–5377 (2014)
213. Warren, D.B., Anby, M.U., Hawley, A., Boyd, B.J.: Real time evolution of liquid crystalline nanostructure during the digestion of formulation lipids using synchrotron small-angle X-ray scattering. *Langmuir* **27**(15), 9528–9534 (2011)
214. Hummer, A.A., Rempel, A.: The use of X-ray absorption and synchrotron based micro-X-ray fluorescence spectroscopy to investigate anti-cancer metal compounds in vivo and in vitro. *Metalomics* **5**(6), 597–614 (2013)
215. Wang, B., Feng, W., Chai, Z., Zhao, Y.: Probing the interaction at nano-bio interface using synchrotron radiation-based analytical techniques. *Sci. China Chem.* **58**(5), 768–779 (2015)

216. Ilinski, P., Lai, B., Cai, Z., Yun, W., Legnini, D., Talarico, T., Cholewa, M., Webster, L.K., Deacon, G.B., Rainone, S., Phillips, D.R., Stampfl, A.P.J.: The direct mapping of the uptake of platinum anticancer agents in individual human ovarian adenocarcinoma cells using a hard X-ray microprobe. *Cancer Res.* **63**(8), 1776–1779 (2003)
217. Wang, B., Yin, J.-J., Zhou, X., Kurash, I., Chai, Z., Zhao, Y., Feng, W.: Physicochemical origin for free radical generation of iron oxide nanoparticles in biomicroenvironment: catalytic activities mediated by surface chemical states. *J. Phys. Chem. C* **117**(1), 383–392 (2013)
218. Wang, L., Li, J., Pan, J., Jiang, X., Ji, Y., Li, Y., Qu, Y., Zhao, Y., Wu, X., Chen, C.: Revealing the binding structure of the protein corona on gold nanorods using synchrotron radiation-based techniques: understanding the reduced damage in cell membranes. *JACS* **135**(46), 17359–17368 (2013)
219. Zhong, J., Song, L., Meng, J., Gao, B., Chu, W., Xu, H., Luo, Y., Guo, J., Marcelli, A., Xie, S., Wu, Z.: Bio-nano interaction of proteins adsorbed on single-walled carbon nanotubes. *Carbon* **47**(4), 967–973 (2009)
220. Robinson, I.: Nanoparticle structure by coherent X-ray diffraction. *J. Phys. Soc. Jpn.* **82**(2), 021012 (2012)
221. Li, X., Chiu, C.-Y., Wang, H.-J., Kassemeyer, S., Botha, S., Shoeman, R.L., Lawrence, R.M., Kupitz, C., Kirian, R., James, D., Wang, D., Nelson, G., Messerschmidt, M., Boutet, S., Williams, G.J., Hartmann, E., Jafarpour, A., Foucar, L.M., Barty, A., Chapman, H., Liang, M., Menzel, A., Wang, F., Basu, S., Fromme, R., Doak, R.B., Fromme, P., Weierstall, U., Huang, M.H., Spence, J.C.H., Schlichting, I., Hogue, B.G., Liu, H.: Diffraction data of core-shell nanoparticles from an X-ray free electron laser. *Sci. Data* **4**, 170048 (2017)
222. Whitesides, G.M.: The origins and the future of microfluidics. *Nature* **442**, 368 (2006)
223. Song, Y., Hormes, J., Kumar, C.S.S.R.: Microfluidic synthesis of nanomaterials. *Small* **4**(6), 698–711 (2008)
224. Salafi, T., Zeming, K.K., Zhang, Y.: Advancements in microfluidics for nanoparticle separation. *Lab Chip* **17**(1), 11–33 (2017)
225. Valencia, P.M., Farokhzad, O.C., Karnik, R., Langer, R.: Microfluidic technologies for accelerating the clinical translation of nanoparticles. *Nat. Nanotechnol.* **7**(10), 623–629 (2012)
226. Björmalm, M., Yan, Y., Caruso, F.: Engineering and evaluating drug delivery particles in microfluidic devices. *J. Contr. Release* **190**, 139–149 (2014)
227. Lo Giudice, M.C., Herda, L.M., Polo, E., Dawson, K.A.: In situ characterization of nanoparticle biomolecular interactions in complex biological media by flow cytometry. *Nat. Commun.* **7**, 13475 (2016)
228. Sun, J., Xianyu, Y., Jiang, X.: Point-of-care biochemical assays using gold nanoparticle-implemented microfluidics. *Chem. Soc. Rev.* **43**(17), 6239–6253 (2014)
229. Fan, X., White, I.M.: Optofluidic microsystems for chemical and biological analysis. *Nat. Photonics* **5**, 591 (2011)
230. Varghese, S.S., Zhu, Y., Davis, T.J., Trowell, S.C.: FRET for lab-on-a-chip devices—current trends and future prospects. *Lab Chip* **10**(11), 1355–1364 (2010)
231. Dannhauser, D., Romeo, G., Causa, F., De Santo, I., Netti, P.A.: Multiplex single particle analysis in microfluidics. *Analyst* **139**(20), 5239–5246 (2014)
232. Stehle, R., Goerigk, G., Wallacher, D., Ballauff, M., Seiffert, S.: Small-angle X-ray scattering in droplet-based microfluidics. *Lab Chip* **13**(8), 1529–1537 (2013)